Aus dem Institut für Schlaganfall- und Demenzforschung
der Ludwig-Maximilians-Universität München
Direktor: Prof. Dr. med. Martin Dichgans

Role of Histone Deacetylase 9 in Pro-Inflammatory Responses in Monocytes and Macrophages

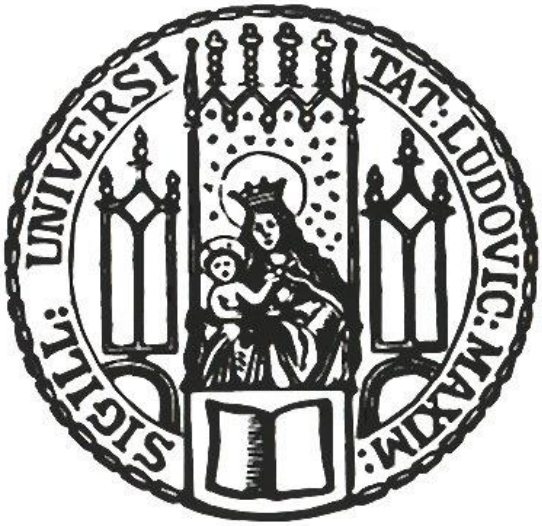

Dissertation
zum Erwerb des Doktorgrades der Medizin
an der Medizinischen Fakultät der
Ludwig-Maximilians-Universität zu München

vorgelegt von
Lydia Luya Yu
aus
Langen, Hessen

2022

Mit Genehmigung der Medizinischen Fakultät
der Ludwig-Maximilians-Universität München

Berichterstatter:	Prof. Dr. med. Martin Dichgans
Mitberichterstatter:	PD Dr. med. Reinhard Obst Prof. Dr. med. Christian Weber apl. Prof. Dr. rer. nat. Aloys Schepers
Mitbetreuung durch den promovierten Mitarbeiter:	Dr. rer. nat. Yaw Asare
Dekan:	Prof. Dr. med. Thomas Gudermann
Tag der mündlichen Prüfung:	10.11.2022

Eidesstattliche Versicherung

Yu, Lydia Luya
_____

Ich erkläre hiermit an Eides statt, dass ich die vorliegende Dissertation mit dem Titel

„Role of Histone Deacetylase 9 in Pro-Inflammatory Responses in Monocytes und Macrophages”

selbständig verfasst, mich außer der angegebenen keiner weiteren Hilfsmittel bedient und alle Erkenntnisse, die aus dem Schrifttum ganz oder annähernd übernommen sind, als solche kenntlich gemacht und nach ihrer Herkunft unter Bezeichnung der Fundstelle einzeln nachgewiesen habe.
Ich erkläre des Weiteren, dass die hier vorgelegte Dissertation nicht in gleicher oder in ähnlicher Form bei einer anderen Stelle zur Erlangung eines akademischen Grades eingereicht wurde.

München, den 10.11.2022

Lydia Luya Yu

_____

Abstract

Background: The histone deacetylase 9 (HDAC9) gene region on chromosome 7p21.1 has been identified as a major risk locus for large-vessel stroke, coronary and peripheral artery disease and atherosclerotic aortic calcification. The pro-atherogenic role of HDAC9 has been well established in experimental mouse models. However, the mechanisms linking HDAC9 to atherosclerosis remain poorly understood.

Methods: Pro-inflammatory responses were studied *in vivo* using peritonitis models in *Hdac9*$^{-/-}$*Apoe*$^{-/-}$ and control littermates and *in vitro* in primary mouse macrophages. The NF-κB signaling pathway was explored by immunoblotting. Furthermore, we investigated the effects of pharmacological class IIa HDAC inhibitor TMP195 on atherosclerosis in *Apoe*$^{-/-}$ mice by immunohistochemistry and examined effects on NF-κB signaling and on human monocyte activation by immunoblotting and ELISA.

Results: We showed that *Hdac9* deficiency results in attenuated inflammation. This was demonstrated by reduced leukocyte recruitment *in vivo* under acute inflammatory conditions and a reduction of pro-inflammatory and pro-atherogenic chemokines and cytokines *in vivo* and *in vitro* in primary as well as peritoneal macrophages. Mechanistically, HDAC9 enhanced p65 phosphorylation at serine residues 536 and 468 in primary macrophages. Treatment with the selective class IIa HDAC inhibitor TMP195 resulted in reduction of pro-inflammatory cytokine production by BMDMs from *Apoe*$^{-/-}$ mice, limited p65 phosphorylation and attenuated atherosclerotic plaque development *in vivo*. Moreover, TMP195 had limiting effects on cytokine production in monocytes from both healthy donors (n=5-6) and patients with established atherosclerosis (n=10-12).

Conclusions: The results demonstrate a pro-inflammatory and pro-atherogenic role of HDAC9 in macrophages and monocytes and identify an activating effect of HDAC9 on NF-κB signaling. Importantly, selective pharmacological inhibition of these HDAC9-dependent mechanisms with the class IIa HDAC inhibitor TMP195 acts as a promising novel therapeutic approach to prevent vascular inflammation.

Zusammenfassung

Hintergrund: Die HDAC9 Gen-Region auf Chromosom 7p21.1 wurde als bisher stärkster genetischer Risikofaktor für ischämische Schlaganfälle der großen Gefäße, Aortensklerose, koronare Herzerkrankung und periphere Gefäßerkrankungen identifiziert. Eine pro-inflammatorische Rolle von HDAC9 in Mausexperimenten ist in der Literatur bereits beschrieben, jedoch bleibt das genaue Verständnis der Mechanismen, welche HDAC9 und Atherosklerose verbinden, weiterhin unvollständig erforscht.

Methoden: Pro-inflammatorische Prozesse wurden *in vivo* mittels des Peritonitis-Modells in *Hdac9*$^{-/-}$*Apoe*$^{-/-}$ Mäusen und *Apoe*$^{-/-}$ Kontrollmäusen und *in vitro* in primären Makrophagen untersucht. Die NF-κB Signalkaskade wurde mittels Western Blot (WB) analysiert. Zudem untersuchten wir immunhistochemisch die Auswirkungen des HDAC IIa spezifischen Inhibitors TMP195 auf atherosklerotische Prozesse in *Apoe*$^{-/-}$ Mäusen, auf den NF-κB Signalweg und auf aktivierende Prozesse in menschlichen Monozyten mittels WB und ELISA.

Ergebnisse: Es konnte gezeigt werden, dass HDAC9-Defizienz unter akut- sowie chronisch-entzündlichen Bedingungen zu einer reduzierten Leukozytenrekrutierung *in vivo* sowie zu einer Reduktion pro-inflammatorischer atherogener Chemokine und Zytokine in primären Makrophagen sowie Peritoneal-Makrophagen führt. Auf molekularer Ebene verstärkt HDAC9 die Phosphorylierung von p65 an den Serinresten 536 und 468 in primären Makrophagen. Bei Anwendung des Klasse IIa HDAC Inhibitors TMP195 zeigte sich in primären Makrophagen ebenfalls eine Reduktion pro-inflammatorischer Zytokine und eine verminderte p65 Phosphorylierung. Zudem führte TMP195 zu einer reduzierten atherosklerotischen Plaquebildung *in vivo* und hat limitierende Auswirkungen auf die Bildung von pro-inflammatorischen Zytokinen in Monozyten von sowohl gesunden Patienten als auch von Patienten mit nachgewiesener Atherosklerose der Karotiden.

Schlussfolgerung: Die Ergebnisse dieser Arbeit demonstrieren die pro-inflammatorische sowie atherogene Rolle von HDAC9 in Makrophagen. Es konnte zudem der aktivierende Effekt von HDAC9 auf den NF-κB Signalweg identifiziert werden. Die selektive Inhibition von Klasse IIa HDACs mittels TMP195 eröffnet eine neue Perspektive für die Prävention von Atherosklerose und inflammatorischen Gefäßprozessen.

Table of Contents

1 Introduction

1.1 Large-vessel stroke

Stroke is defined as an acute focal damage of the central nervous system resulting in a sudden neurological deficit caused by a vascular pathology [1]. According to the Global Burden Disease Study of 2016, stroke is the second most common cause of death worldwide (10% of all deaths) [2] with a global lifetime risk from the age of 25 years onward of 25% among both men and women [3]. Moreover, stroke is the second most common cause for disability-adjusted life years (DALYs) (5% of all DALYs worldwide), which describes the sum of years of life lost due to premature mortality plus years lived with disability [4]. In Germany, about 200.000 first-ever and approximately 66.000 recurrent strokes occur each year [5]. In the classification of stroke subtypes, the more common ischemic stroke (~80%) has to be distinguished from hemorrhagic stroke (~20%) and unspecified stroke [6]. While the cease of blood circulation in a hemorrhagic stroke is result of vessel rupture with extravasation of blood, ischemic stroke is characterized by embolus or thrombus causing occlusion of a cerebral vessel or brain supplying artery. According to the Trial of ORG 10172 in Acute Stroke Treatment (TOAST) classification of ischemic stroke, there are five different subtypes which consist of large-vessel stroke (LVS), cardioembolic stroke, small vessel stroke, other determined etiology and undetermined etiology [7] (Figure 1).

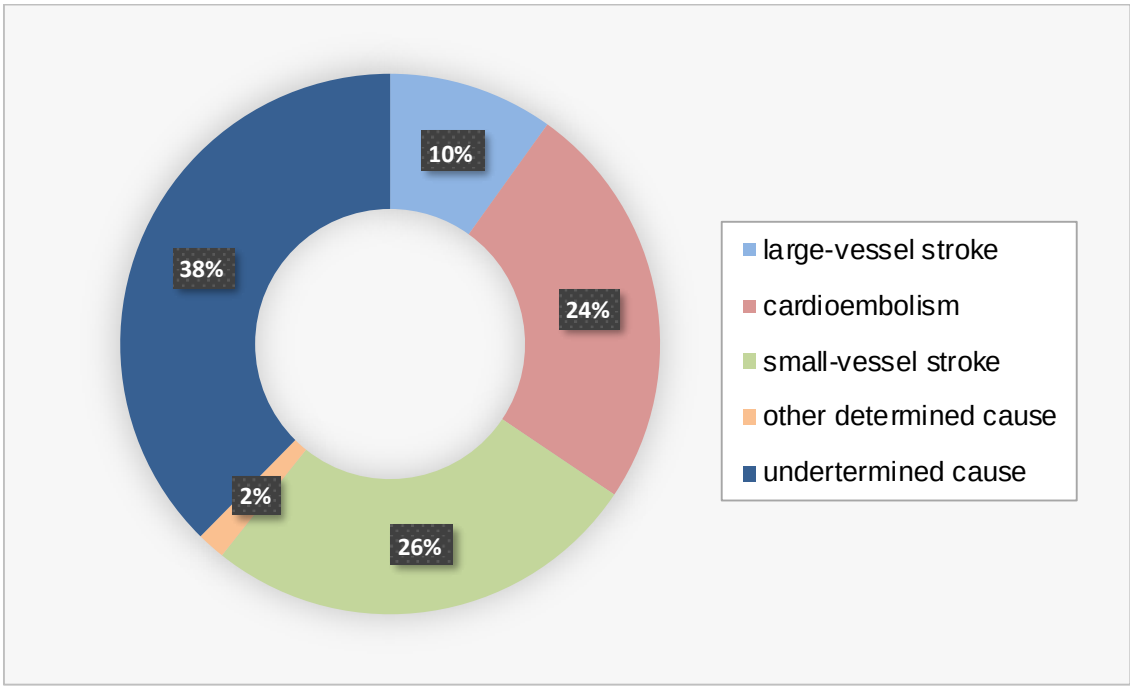

Figure 1. Subtypes of ischemic stroke in German study population from 1995-2010

Ischemic stroke etiology can be classified according to the TOAST classification with 10% large-vessel stroke, 24% cardioembolism, 26% small-vessel stroke, 2% other determined cause such as fibro-muscular dysplasia or dissection and 38% undetermined cause. (Figure generated with data from the Erlangen Stroke Project 1995-2010, Kolominsky-Rabas et al. [8])

About a quarter of all stroke patients (ischemic and non-ischemic) suffer from LVS, which are attributed to atherosclerosis in the vessel wall of the carotid and cerebral arteries [9]. While there are modifiable risk factors like hypertension, diabetes or nicotine combined with acquired risk factors like age, gender and ethnicity, there are also strong heritable components that add to this heterogeneous and multifactorial disease. Many of these risk factors of LVS also increase coronary artery disease (CAD) and peripheral artery disease (PAD) [10, 11], which emphasizes atherosclerosis as the common underlying disease. Since risk factors and heritability of ischemic stroke are different amongst stroke subtypes, with estimated 40.3% heritability for LVS, 32,6% for cardioembolism and only 16.1% for small vessel disease, ischemic stroke subtyping is crucial for genetic association studies [12].

1.1.1 7p21.1 as risk locus for large-vessel stroke

Recent genome wide association studies (GWAS) have identified the histone deacetylase (HDAC9) gene region on chromosome 7p21.1 as the most prominent

risk locus for LVS [13-15], and a major locus for CAD [11, 16] as well as PAD [17] and atherosclerotic aortic calcification [18]. In a collaborative meta-analysis of ischemic stroke genome-wide association studies (METASTROKE), rs2107595 was confirmed as the lead single-nucleotide polymorphism (SNPs) for the LVS subtype [14]. SNPs are the most common kind of genetic variation among the human DNA and occur when a single nucleotide is replaced with another. Most of these variants have no genetic consequences, however, if located in coding regions or regulatory regions, some may cause altered gene expression with possible increase of disease risk. In this case, rs2107595 is localized in the intergenic region at the 3'-end of the *HDAC9* gene and 100kb upstream to the next 2 genes *TWIST1* and *FERD3L* [9]. Elevated HDAC9 expression, but not TWIST1 and FERD3L was found in risk allele carriers of the lead SNP, indicating that effects at this variant is mediated through increased expression of HDAC9 [9]. However, the exact functional mechanisms by which HDAC9 alters disease risk are yet to be elucidated.

1.2 Atherosclerosis

Atherosclerosis is a chronic inflammatory disease of large and medium-sized arteries, mostly found at predilection sites with blood flow turbulences like branch arteries [19]. It is the underlying pathogenesis not only of ischemic stroke, but also of other cardiovascular diseases (CVD) such as coronary artery disease (CAD) and peripheral artery disease (PAD), and thus the leading cause of death and morbidity worldwide [20, 21]. For instance, in the year of 2012, CVD was responsible for 43.9% of deaths in women and 36.1% in men in Germany [22]. Atherosclerosis is characterized by a multifactorial development of chronic endothelial dysfunction influenced by hemodynamics, genetics, imbalanced lipid metabolism and maladaptive chronic immune response [23, 24], which result in lesion formation that protrude into the arterial lumen [25]. Multiple cell types are involved in atherogenesis including vascular cells like endothelial cells (ECs) and smooth muscle cells (SMCs) and cells from both the innate and adaptive immune system. Besides monocytes and macrophages, recruited cells during the inflammatory cascade also encompass the leukocyte subsets of neutrophils, T cells, B cells, dendritic cells and mast cells as well as platelets [26].

1.2.1 Stages in development of atherosclerosis

The development of atherosclerosis can be categorized into four consecutive steps (Figure 2):

A) *Lesion Initiation.* In the initial stage of atherogenesis, dysfunction of the vascular wall is caused by a variety of risk factors like alteration of blood flow or imbalance in lipid metabolism with accumulation of low-density lipoprotein (LDL) in the intima [24, 27]. This leads to activation of the endothelial cells which results in secretion of adhesion molecules like vascular cell adhesion molecule-1 (VCAM-1) and intercellular adhesion molecule-1 (ICAM-1), chemokines like monocyte chemotactic protein-1 (MCP-1), macrophage migration inhibitory factor (MIF) and TNF-α and growth factors like macrophage colony-stimulating factor (MCSF) [28]. As a result, permeability of the vessel wall is increased with recruitment and transmigration of leukocytes into the tunica intima [27]. Recruited leukocytes mostly include circulating monocytes and also various other cell types such as neutrophils, B-cells, T-cells as well as platelets, dendritic cells and mast cells [20]. Recruited monocytes proliferate and differentiate into macrophages [29] while LDL particles in the vessel wall get modified by oxidation resulting in oxidized LDL (oxLDL).

B) *Early lesion (fatty streak).* Under inflammatory conditions induced by chemokines like CCL2, CCL8, CXCL1, IL1-β and TNF-α, more leukocytes are recruited and macrophages turn into foam cells through rapid phagocytosis of cholesterol. This results in sustained secretion of pro-inflammatory chemokines and other cytokines [20] with constant contribution to the chronic state of vessel inflammation. Eventually, this leads to the development of early lesions called “fatty streaks”, a key step of atherosclerosis [27, 30].

C) *Mature fibrous plaque*. Here, activated inflammatory immune cells, cell death and increasing amounts of extracellular lipids result in growing masses of intimal fibroatheromatous plaques [27]. These plaques are covered by a fibrous cap consisting of migrated SMC from the tunica media, which proliferate and produce collagen. Necrosis of macrophages contribute to formation of lipid-rich necrotic cores resulting in so called vulnerable or unstable plaques [23].

D) *Rupture and thrombosis*. In the advanced stages of atherogenesis, plaque growth gradually leads to reduced blood flow and vessel stenosis. Simultaneously, weakened plaque stability may lead to rupture of the thinning fibrous cap with exposed prothrombotic material for local thrombosis or distant artery embolism [20]. Together, this results in clinical manifestations such as stroke and transient ischemic attacks (TIA), acute coronary syndrome (CAD) like myocardial infarction and other diseases like hypertension or critical limb ischemia.

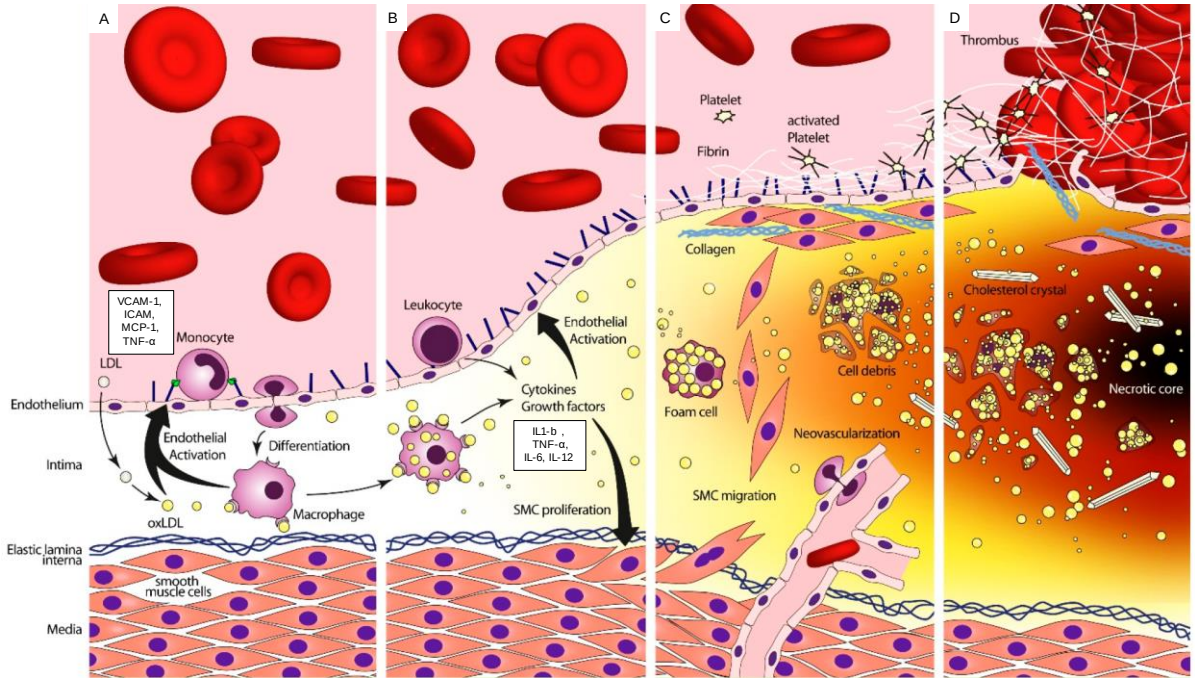

Figure 2. Stages of atherosclerosis development.

A) In the initial stage, after endothelial activation by LDL accumulation in the subendothelial matrix, monocytes are recruited and migrate into the tunica intima to differentiate into macrophages. B) Macrophages develop into foam cells by rapid oxLDL uptake and form „fatty streaks “. Concurrently, activated macrophages secrete pro-inflammatory cytokines and chemokines for further leukocyte recruitment, SMC activation and progressed inflammation. C) Smooth muscle cells migrated from the tunica media produce collagen and form fibrous caps while activated platelets adhere to the vessel wall to alter chemotactic and adhesive properties of ECs. D) Necrosis of foam cells result in lipid-rich necrotic core with cell debris and cholesterol crystals that destabilize the plaques and eventually lead to rupture with stenosis, thrombosis or embolism. (Figure modified from Steinl et. al, [31])

1.2.2 Role of monocytes and macrophages in atherosclerosis

Accumulation of leukocytes from both innate and adaptive immune system play a major role in the pathophysiology of atherosclerosis. Especially monocytes and macrophages stand out as key drivers in the pathogenesis of atherosclerosis [32].
A wide range of chemokines and cytokines determine recruitment, function and activity of monocytes as precursor cells of macrophages. In the initial steps of leukocyte recruitment, CCL5 and CXCL1 on ECs interact with receptors of the monocyte surface and ultimately lead to capture, rolling and transmigration [23, 33, 34]. Monocytes then differentiate into macrophages driven by MCSF produced by ECs and SMCs [35]. In the arterial wall, scavenger receptors expressed on macrophages bind modified LDL resulting in foam cell formation which then secrete chemokines CCL2, CCL5, CXCL1 and cytokines IL-1, IL-6 and TNF-α. This ultimately leads to activation of monocytes in the plaque with their polarization into different phenotypes. Monocytes are classified into classical Ly6C^{high} and non-classical Ly6C^{low} based on their cell surface markers [36]. Ly6C^{high} monocytes are known to be pro-inflammatory and express high levels of CC-chemokine receptor 2 (CCR2). They increase under hyperlipidemic conditions and in early atherosclerosis [37]. In contrast, Ly6C^{low} monocytes are believed to have homeostatic and anti-inflammatory functions [23, 38]. Macrophages have been broadly described to have two states- M1 (classically activated) and M2 (alternatively activated) [39]. Initially postulated, M1 macrophages derive from Ly6C^{high} monocytes, secrete pro-inflammatory cytokines like IL-6, IL-12 and TNF-α and therefore promote plaque inflammation. Alternatively activated M2 macrophages are believed to derive from Ly6C^{low} monocytes, produce anti-inflammatory cytokines such as IL-10 and TGFβ and resolve plaque inflammation [40, 41]. However, there has been a recent paradigm shift. It was shown that resolution of inflammation and plaque regression depend upon the recruitment of Ly6C^{high} monocytes, which then acquire the qualities of M2 macrophages [42]. This shows that the Ly6C^{high} subset is not solely the inflammation-prone precursors of M1 macrophages but rather also contribute to plaque regression and inflammation resolution. Nonetheless, the regulation of M1 and M2 balance and their origin remains incompletely and also inconsistently defined and yet to be further elucidated.

Another reason, why macrophages and monocyte-derived cells have a protagonist role in atherosclerosis is that they show impaired resolution of inflammation. Physiologically, macrophages are of great importance for resolution of inflammation and tissue repair by removing apoptotic and necrotic cell debris [43, 44]. In atherosclerosis, however, there is lack of negative feedback of uptake and diminished cell emigration with cell accumulation [45]. Moreover, macrophage apoptosis and necrosis in plaques lead to plaque destabilization with critical influence on risk for rupture and thus clinical manifestation of atherosclerosis [46].

1.2.3 Mouse models of inflammation

Currently, murine models of atherosclerosis are the most frequently used models to study the process of atherogenesis. Although mice are more likely to develop atherosclerotic plaques in the aortic root instead of the coronary arteries and plaque types are more stable with less risk of rupture, these models are still the most widely used [47]. The advantages of murine models over other animal models include low costs of purchase, easy breeding and maintenance and possibility of straightforward genetic manipulation by knock out or replacement of endogenous genes [47]. The most frequently used models of atherosclerosis are *apolipoprotein E (Apoe)*- or the *LDL receptor (LDLR)*-deficient mice, which induce a state of hyperlipidemia, the main risk factors of atherosclerosis. Normally, mice fed with normal low-fat diet do not get atherosclerosis due to their natural HDL-high and LDL-low lipid profile [48]. In *Apoe*-deficient mice, hypercholesterolemia and lesion development can occur spontaneously even when feeding a low-fat chow diet [49, 50], while the *LDLR*-deficient mice require western type diet (WTD) containing 21% fat [51] to develop plaques. When feeding *Apoe*$^{-/-}$ mice this WTD, fibrous plaque development is greatly accelerated with lesions to be found after already 15 weeks compared to 20 weeks in chow diet fed mice (Figure 3) [52]. This allows experimental monitoring of atherogenesis in a reasonable time frame.

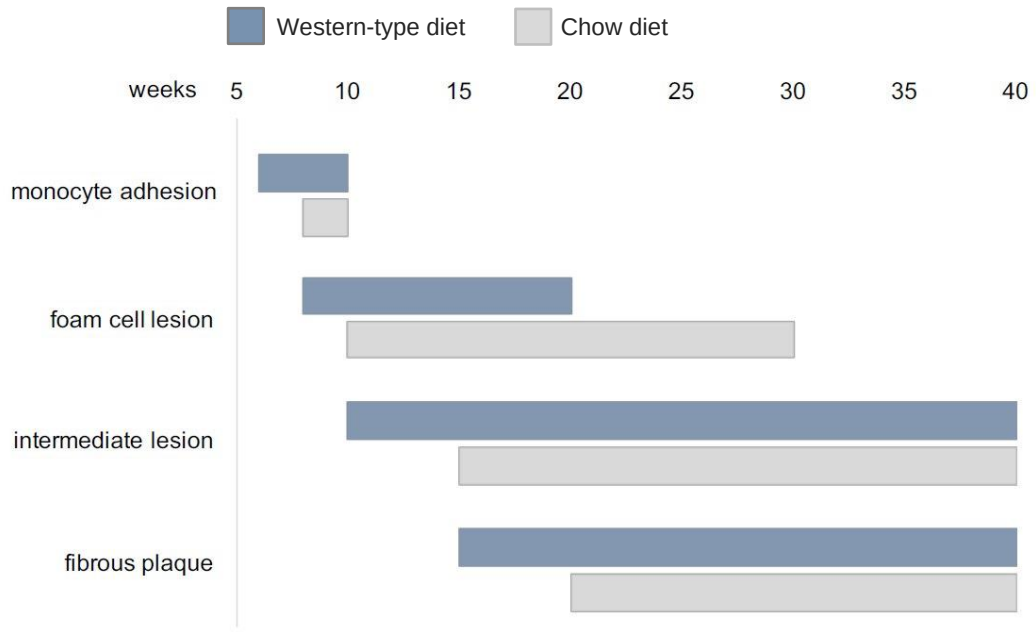

Figure 3. Diet-dependent atherosclerotic lesion development in *Apoe*-deficient mice.

Graph shows accelerated, earlier timepoints of lesion development in mice fed with high fat Western-type diet compared to mice with standard chow diet. For the latter, the graph shows delayed, but still spontaneous atherosclerotic lesion development (Graph adapted from Nakashia et al., [52]).

1.3 Histone deacetylases (HDACs)

1.3.1 HDAC classification and function

Histones are key components of chromatin and act as major regulators of gene expression. Positively charged basic amino acids within the N-terminal domains of histones enable chromatin condensation through interaction with the negatively charged DNA backbone. This silences gene transcription by making the DNA inaccessible for protein binding. Chromatin structure and accessibility to DNA can be controlled by posttranslational histone modification such as acetylation and methylation [53]. Especially histone acetylation plays a crucial role in transcriptional regulation. It is a dynamic process controlled by the enzymes histone acetyltransferases (HATs) and histone deacetylases (HDACs). HATs acetylate histone lysine residues and neutralize the positive charge. This leads to relaxation of the chromosome structure, thus increasing accessibility and transcription activity. In contrast, HDACs allow chromatin compaction and increase transcriptional repression

by removing lysine acetylation and increasing the ionic interaction between the positively charged histones and the negatively charged DNA (Figure 4).

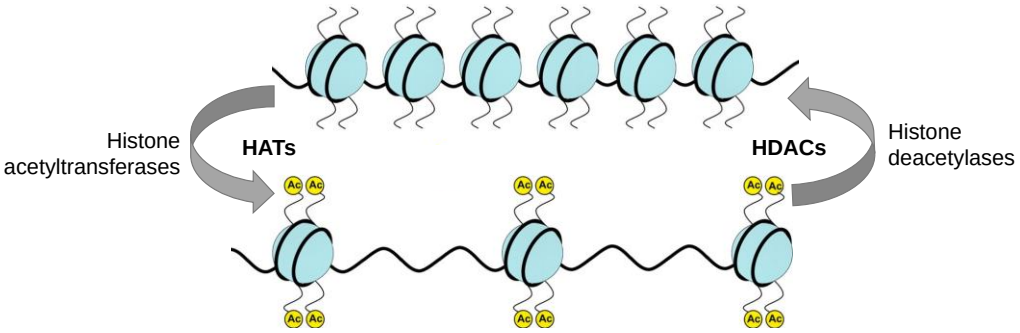

Figure 4. Histone deacetylases and histone acetyltransferases.

Histone acetylation and deacetylation are controlled by two antagonistic enzyme families, the histone deacetylases and the histone acetyltransferases. In the deacetylated state, interaction between positively charged ε-amino groups of lysine residues and negatively charged DNA backbone leads to chromatin compaction and transcriptional repression. Acetylation of these groups disrupt interaction and results in relaxed chromatin accessible to transcription. (Figure adapted from Eslaminejad et. al. [54])

Histone deacetylases (HDACs) are a heterogenic family of enzymes that detach an acetyl group from lysine residues of target proteins and have broad regulative effects on various cellular processes and pathogenesis of diseases. More specifically, HDACs have important roles in gene expression, innate immunity [55, 56] and atherosclerosis [28, 57]. Besides histones, HDACs also interact with transcription factors and numerous other non-histone proteins directly. In fact, global analysis in human cells found more than 1750 proteins which contain lysine side chains that can be acetylated [58]. Since lysine residues can also be modified in various other ways, different modification systems lead to signaling crosstalk with multifarious effects on inflammatory and immune responses [55].

The 18 known HDACs, found in both human and mice, can be grouped into four classes which can further be categorized into classical HDACs (class I, IIa, IIb and IV) and sirtuins (class III). The classification is based on sequence homology and domain organization. While class I (HDAC1, 2, 3 and 8), IIa (HDAC 4, 5, 7 and 9), IIb (HDAC 6 and 10) and IV (HDAC 11) are Zn^{2+} dependent enzymes, class III enzymatic

activity requires NAD^+ as cofactor [55]. Class I HDACs are predominantly localized in the nucleus due to nuclear localization sequences and can be found ubiquitously. They have been well studied and play important roles as histone modifiers with high affinity to histone substrates [59], thus having strong repressive influence on gene transcription. Class IIa HDACs have large binding sites in the N-terminal domain that interact with transcriptional repressors and activators such as Hdac9 with repressive effects on the activity of myocyte enhancer factor 2 (MEF2) [60]. Localization of these HDACs is dependent on phosphorylation by kinases which results in their shuttling between nucleus and cytoplasm. In comparison to class I HDACs, most class IIa HDACs possess less deacetylation activity against histones and show more restricted tissue distribution (Table 1). They mostly function by recruiting class I HDACs or other proteins (corepressors or coactivators) [55]. For example, HDAC3 interacts with class II HDACs in the process of endothelial cell proliferation and atherosclerosis [61].

Table 1. Overview of HDACs with their tissue expression pattern, subcellular localization and function. [28, 55, 59, 62, 63]

Class	HDAC	Tissue expression pattern	Subcellular localization	Enzymatic Function
I	1, 2	Ubiquitously expressed	Predominantly in the nucleus	High enzymatic activity toward histone substrates
	3, 8		Ubiquitously in cytoplasm and nucleus	
IIa	4	Brain, growth plates of skeleton	Shuttling between nucleus and cytoplasm	Mostly noncatalytic recruitment of class I HDACs through C-terminal domain and interaction with other transcriptional corepressors or coactivators; HDAC9 promotes TANK-binding kinase-1 (TBK1) kinase activity via its deacetylation
	5	Muscle, heart, brain		
	7	Endothelial cells and thymocytes		
	9	Muscle, heart, brain		
IIb	6	Heart, liver, placenta, kidney	Predominantly cytoplasm	Main cytoplasmic deacetylase
	10	Liver, kidney, spleen		unclear
IV	11	Brain, heart, muscle, kidney, testis	Nucleus	unclear

1.3.2 Histone deacetylase 9 (HDAC9)

Histone deacetylase 9 (HDAC9) is a class IIa HDAC involved in cell differentiation [64], proliferation [65], angiogenesis [66], glucose and lipid metabolism [67, 68] and antiviral innate immunity [63]. It is expressed in various atherosclerosis-relevant cells like macrophages [67], smooth muscle cells and vascular endothelial cells [55, 66, 69] and mainly found in brain, heart and skeletal muscle tissue [69]. Unlike other class IIa HDACs, HDAC9 has been shown to have direct enzymatic activity through deacetylation to act as a kinase activator. In fact, HDAC9 enhances TBK1 activity in macrophages by deacetylation of Lys241 during viral infection to enhance antiviral innate immune response [63]. Other, mostly repressive functions result from recruitment of other HDACs like HDAC3 or direct interaction with gene transcription factors like MEF2, a central regulator of diverse developmental programs like VSMC proliferation [60]. MEF2-interacting transcription repressor (MITR) is a splice variant of HDAC9 without the HDAC domain. Notably, repression of MEF2-target genes by MITR is as effective as by the full-length HDAC9 protein which indicates that intrinsic catalytic activity is not a necessity for repression [70, 71].

The HDAC9 protein is known to play an important role in heart development and myogenesis. More specifically, HDAC9 was shown to be essential for suppressing cardiac hypertrophy [72], which was studied with global *Hdac9*-deficient mice first generated by the group of Eric N. Olsen in 2002. Besides the previously mentioned association of the *Hdac9* gene region to LVS, CAD, atherosclerotic aortic calcification and PAD, the 7p21.1 locus has also been linked to carotid intima-media thickness and asymptomatic carotid plaque presence in community populations [69]. Several studies suggest that the effects of the *Hdac9* locus on atherosclerosis risk might be mediated through elevated HDAC9 expression. In fact, in risk alleles carriers, *HDAC9* mRNA expression was shown to be elevated in peripheral blood mononuclear cells with a gene dosage effect [9, 73] and HDAC9 plasma levels were also found elevated [73]. Moreover, HDAC9 shows upregulated mRNA expression in human atherosclerotic plaques of different arteries (carotid, aortic and femoral) [69]. In addition, *Hdac9* deletion in macrophages was shown to suppress cholesterol efflux and to generate alternatively activated macrophages by phenotype switch from M1 to M2 states [67]. Collectively, there is substantial evidence for a pivotal role of HDAC9

in inflammation and atherogenesis. However, the molecular mechanisms linking HDAC9 to atherosclerosis remain poorly defined.

1.3.3 HDAC inhibitors (HDACi)

HDACs are known to be involved in the pathophysiology of various diseases such as cardiovascular diseases, metabolic disorders, autoimmunity and cancers [74-77]. Hence, HDAC inhibitors might represent promising and potential treatment targets.
HDAC inhibitors such as pan-inhibitor suberoyl anilide bishydroxamide (SAHA) and class I inhibitor FK288 are already in clinical use for treatment of cutaneous T-cell lymphoma and valproic acid for epilepsy and bipolar disorder [55]. Many others have beneficial effects on different inflammatory diseases including arthritis, inflammatory bowel disease, graft versus host disease or septic shock [78] in preclinical studies. However, due to the pleiotropic effects of different HDACs, some of those broad-spectrum inhibitors also display evidence of contraindications, as described for trichostatin A (TSA)-induced exacerbation of atherosclerosis in LDLR-deficient mice [79]. Hence, to limit side effects, development of more selective HDAC inhibitors is of high scientific and clinical interest.
For class IIa HDACs, there is still lack of potent and selective inhibitors. This is due to their poorly understood catalytic activity and also based on the pharmacological limitations of zinc-chelating groups used in most metalloenzyme inhibitors [80]. Fortunately, recent studies introduced a series of first-in-class selective class IIa histone deacetylase inhibitors via a nonchelating zinc-binding group that specifically occupy and block the acetyllysine-binding site of HDAC 4, 5, 7 and 9 [80]. Out of all introduced inhibitors, TMP195 is the most promising and potent candidate for HDAC9 inhibition with a very low inhibition constant value (K_i) of 0.015, which represents its high inhibition efficiency to HDAC9 [81]. More importantly, TMP195 was successfully used *in vivo* in mice with a reduction of breast tumor burden and metastases by modulation of macrophage phenotype without any significant evidence of cytotoxicity [81]. Therefore, TMP195 is a promising potential pharmacological approach for anti-inflammatory therapy and has been a major focus of this study.

1.4 Nuclear factor kappa-light-chain-enhancer of activated B cells (NF-κB)

The transcription factor Nuclear factor kappa-light-chain-enhancer of activated B cells (NF-κB) was first discovered 1986 in the laboratory of David Baltimore [82] and is a well-known master regulator of inflammation. Many pro-inflammatory genes that drive atherosclerosis such as chemokines, cytokines, adhesion molecules and growth factors like CCL2, CXCL1, IL1-β, IL-6 or TNF-α [83] are known to be regulated by NF-κB. Hence, with more than 160 NF-κB-regulated genes, multifarious responses in innate and adaptive immunity are dependent on NF-κB regulation [83]. On the one hand, NF-κB plays a fundamental role in many physiological processes such as regulation of epithelial function, muscular and skeletal systems and most importantly the homeostasis of the immune system as regulator of cell survival, proliferation and apoptosis [84, 85]. On the other hand, NF-κB dysregulation is involved in many inflammatory diseases including atherosclerosis, cancer, neurodegeneration and auto immunity [86-88].

NF-κB consists of a small protein family with five members: p65 (Rel-A), Rel-B, c-Rel, p50 (and its precursor p105) and p52 (and its precursor p100), which together may form more than twelve different hetero- and homo-dimers [89]. The most abundant dimer is the p65/p50 complex. All subunits are partly made of the N-terminal Rel Homology Domain (RHD) which controls dimerization, protein interaction as well as DNA binding. Only the three subunits p65, Rel-B and c-Rel additionally consist of a transactivation domain (TAD) controlling their transcriptional activity. In contrast, p50 and p52, after proteolytic processing of their larger precursor proteins p105 and p100, act as repressors without any transcriptional activity.

1.4.1 Signaling pathway

There are two known pathways for NF-κB activation - the canonical pathway (Figure 5) and the non-canonical pathways. In unstimulated resting cells, NF-κB is kept inactive in the cytoplasm through interaction with the inhibitory IκB protein family, mostly through direct binding to the most predominant and best studied isoform IκB-α. Multiple signals are known to activate either one or both of the pathways. The canonical pathway can be induced by TNF-α, IL1-β, Lipopolysaccharide (LPS) or other extracellular stimuli such as viral products or bacterial components [90]. These

stimuli bind to receptors such as the tumor necrosis factor receptor (TNFR), innate pattern-recognition receptors like Toll-like receptors (TLRs) or antigen receptors [83]. The subsequent cascade involving different upstream protein complexes, such as the TNFR-associated factors (TRAF), essentially leads to the activation of the IκB kinase (IKK) complex which consist of the two catalytic subunits IKKα and IKKβ and the regulatory subunit IKKγ (also called NEMO). Signal-dependent phosphorylation of IκB-α by the IKK complex marks it for SCF-βTrCP-dependent polyubiquination and ubiquitin-mediated proteolysis [91], which ultimately frees the NF-κB complex for translocation to the nucleus. There, NF-κB binds to specific DNA sequences for activation of transcription.

Due to its pleiotropic effects on physiological as well as pathological processes, NF-κB has to be tightly regulated to ensure the correct termination of its activity to prevent any dysregulation resulting in inflammation, autoimmune disease and oncogenesis [92]. One of such regulatory mechanisms is a negative-feedback loop via NF-κB-induced IκB-α synthesis [93] (Figure 5). Newly synthesized IκB-α enters the nucleus and binds to activated NF-κB [94], followed by translocation of the NF-κB-IκB-α complex back to the cytoplasm, resulting in termination of NF-κB transcription activity. Moreover, NF-κB DNA-binding subunits are subject to regulation by post-translational modifications (PTMs), such as phosphorylation, acetylation, methylation or ubiquitination. These PTMs affect the interaction of NF-κB with coactivators, corepressors, IκB proteins and transcription factors [90]. For example, phosphorylation status of p65 determines its association with CREB binding protein and its homolog p300 (CBP/p300), an important transcription coactivator possessing histone acetyltransferase activity [95]. Hence, PTMs are crucial for possible cross-links and integration of non-NF-κB pathways. For class I HDACs (HDAC 1, 2 and 3), studies have previously described their direct interaction with the subunit p65 in the nucleus with repressive effects on NF-κB activity [95-97]. In contrast, the exact mechanisms linking class IIa HDACs, particularly HDAC9, to the NF-κB signaling pathway remain to be defined. Possible links could be through IKKα, IKKβ, or non-canonical kinases TBK1 and IKKε, which are all kinases that phosphorylate the subunit p65 [63, 98].

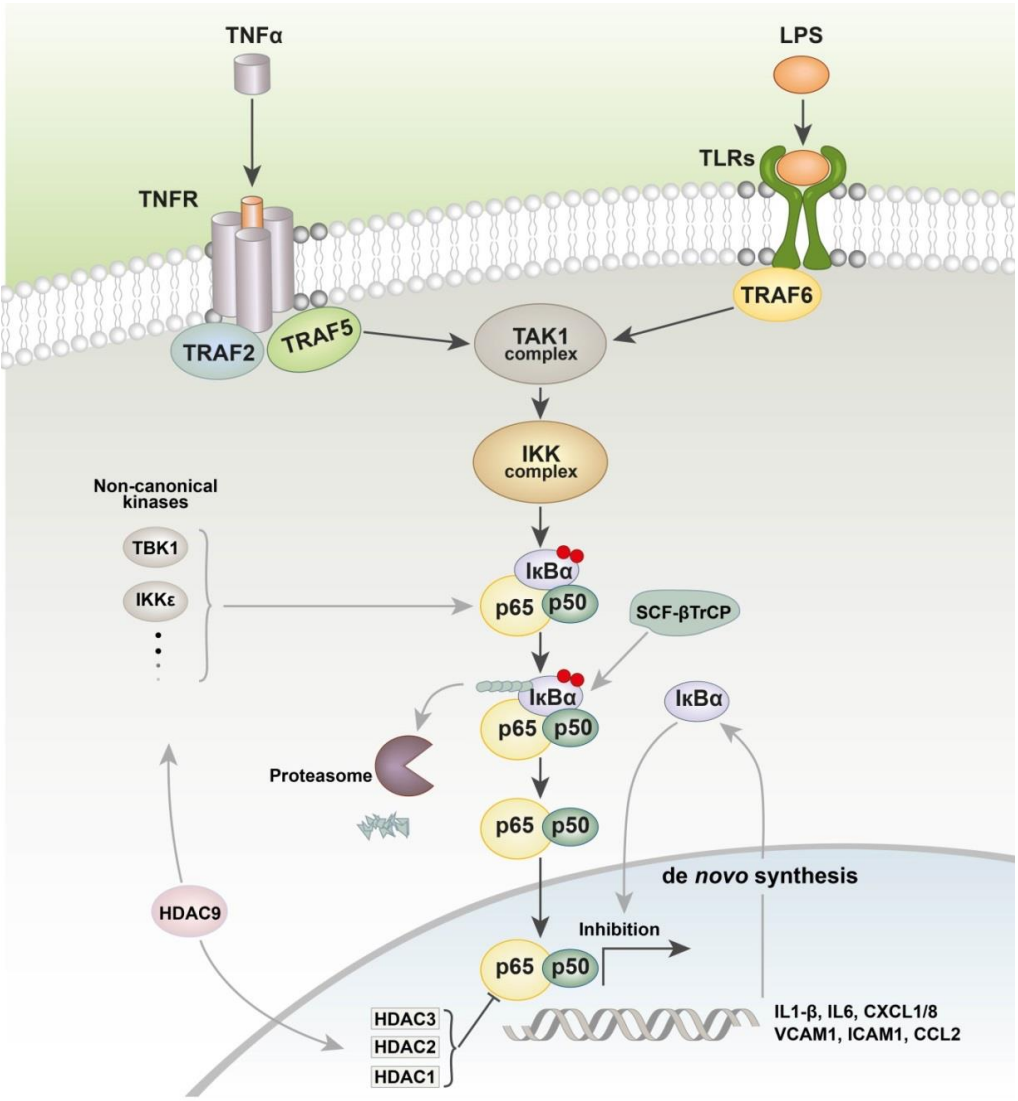

Figure 5. NF-κB activation of canonical signaling pathway.

Schematic representation of the classical activation pathway of NF-κB upon TNFR and TLR-dependent stimulation with TNF-α and LPS depicted as the exemplary stimuli. The subsequent signal cascade involves several kinase complexes including TRAFs, TAK1 and the IκB-kinases (IKKs) which eventually results in translocation of the IκB-α-freed NF-κB complex into the nucleus. This enables DNA binding and activates gene transcription of NF-κB-regulated genes like IL1-β, IL6, CXCL1 and CCL2. Being tightly downregulated, the active NF-κB complex can either be repressed by IκB-α as part of a negative feedback loop or amongst others be deactivated by association with class I HDACs. Possible crosslinks of HDAC9 to non-canonical kinases like IKKα, IKKβ, TBK1 or IKKε are yet to be further explored (Figure by Asare et. al., unpublished).

In the alternative pathway (not depicted in the figure), IKKα and the NF-κB-inducing kinase (NIK) selectively regulate the proteolytic processing of p100 to p52 for modulation of the transcriptional active heterodimer p65-p52. In resting cells p100 is kept inactivated in the cytoplasm, while upon stimulation with LTβ, CD40 ligand or LPS the p65-p52 complex can translocate to the nucleus und activate transcription. Since the alternative pathway is mostly associated with the development and survival of B-cells [99], it is not further elaborated in this study.

1.4.2 Phosphorylation of NF-κB

NF-κB subunits are accessible to various kinds of PTMs and the most well studied form is phosphorylation, which is known to play a crucial role in regulation, function and activity of NF-κB. The modulating, enhancing or downregulating effects are dependent on the specific site of phosphorylation of the five subunits [84]. In particular, phosphorylation of the subunit p65 has been extensively described to regulate the activity of NF-κB. There are multiple residues of p65 known to be phosphorylated either in the rel homology or in the transactivation domain (Figure 6).

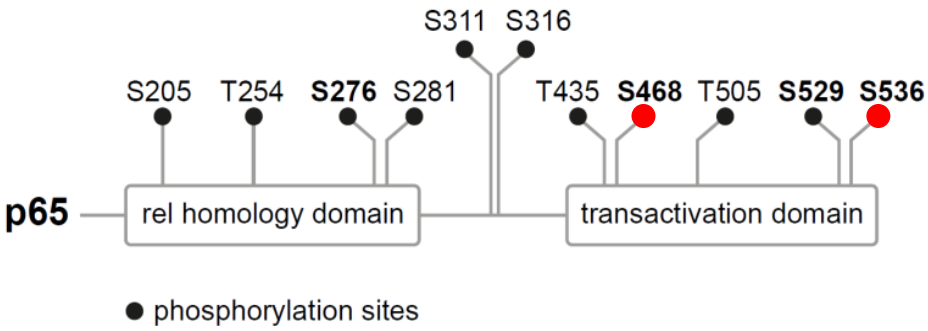

Figure 6. Schematic diagram of p65 structure and phosphorylation sites.

This diagram depicts the principal structural motif of subunit p65, which include the REL homology domain (RHL) and the transactivation domain (TAD). All known phosphorylation sites are shown. This study mainly focused on serine residues S468 and S536. (Figure adapted from Christian et. al. [84])

Since each residue has specific kinases that are known to phosphorylate them, resulting in enhancing or inhibitory effects on NF-κB activity (Table 2), a target gene-specific manner ('barcode hypothesis') of transcription can be postulated [98]. In other words, each NF-κB inducing stimulus leads to the activation of a very specific set of NF-κB target genes.

Our study focuses on the two well-studied serine residues S536 and S468 located in the C-terminal TAD. While S536-phosphorylated p65 mainly localizes in the cytosol, S468-phosphorylated p65 can be predominantly found in the nucleus [98]. Kinases that phosphorylate p65 at S536 include IKKβ, ribosomal subunit S6 kinase 1 (RSK1), IKKα, IKKε and NAK/TBK1 [100].

Phosphorylation of S536 leads to enhancement of NF-κB transactivation, which was shown to be mediated through increased p65 acetylation at K310 [101]. Furthermore, phosphorylated p65 has a lower affinity for IκB-α which allows increased translocation to the nucleus [84]. For S468 phosphorylation, there are three known kinases with differential effects on p65 activity. While GSK3β leads to reduced basal NF-κB activity [102], IKKε mediated phosphorylation enhances transactivation [103]. IKKβ phosphorylation of S468 leads to proteasomal degradation of p65, thus having an overall limiting effect on gene transcription [104, 105].

Table 2. Phosphorylation and associated kinases of p65 serine 536 and serine 468 [84]

Site	Kinase	Effect	Source
S536	IKKβ	For all kinases: transactivation and K310 acetylation	[100, 106]
	RSK1		[100]
	IKKα		[100, 106, 107]
	IKKε		[100, 108]
	NAK/TBK1		[100]
S468	GSK3β	inhibition	[102]
	IKKε	transactivation	[103]
	IKKβ	slight inhibition	[104]

1.5 Aim of the study

The histone deacetylase 9 (HDAC9) gene region on chromosome 7p21.1 has been identified as a major risk locus for large-vessel stroke, coronary artery disease, atherosclerotic aortic calcification and peripheral artery disease. Moreover, elevated *HDAC9* expression levels as well as elevated HDAC9 plasma levels in human atherosclerosis suggest its distinct pro-atherogenic role. However, the mechanisms linking HDAC9 to vascular inflammation and the subsequent therapeutic potential remain poorly defined.

The aims of this thesis are:

(1) to explore the mechanisms linking HDAC9 to atherogenesis by employing *in vivo* mouse models of acute and chronic inflammation as well as *in vitro* studies. The thesis specifically focuses on the pro-inflammatory effects of HDAC9 on chemokine and cytokine production in monocytes and primary macrophages;

(2) to identify downstream signaling pathways mediating these responses;

(3) to explore the therapeutic potential of recently reported selective competitive class IIa HDAC inhibitor TMP195 for atheroprotection.

2 Materials

2.1 Equipment

Table 3: List of used equipment

Equipment	Company
AutoMACS Pro Separator	Miltenyi (Bergisch Gladbach, GER)
Automated cell counter TC20	BIO-RAD (Hercules, US)
Biological Safety Cabinet HERAsafe KS	Thermo Scientific (Waltham, US)
Block Heater SHT100D	Stuart Scientific (Staffordshire, UK)
Centrifuge 5415 D	Eppendorf (Hamburg, GER)
Centrifuge 5427 R	Eppendorf (Hamburg, GER)
Centrifuge 5810R	Eppendorf (Hamburg, GER)
Centrifuge Herareus Megafuge 16	Thermo Scientific (Waltham, US)
Centrifuge Herareus Megafuge 16 R	Thermo Scientific (Waltham, US)
Centrifuge Perfect Spin 24	PEQLAB (Erlangen, GER)
Counting chamber, Neubauer	Marienfeld (Königshofen, GER)
Cryostat Leica CM1950	Leica (Wetzlar, GER)
Electrophoresis power supply PeqPower300 PowerPac HC	 PEQLAB (Erlangen, GER) PEQLAB (Erlangen, GER)
Electrophoresis system Mini-PROTEAN Tetra	BIO-RAD (Hercules, US)
Elmasonic S 10 H	Elma (Fremont, US)
Freezer -20°C	Liebherr (Bulle, CH)
Freezer -80°C Hera Freeze Basic	Thermo Scientific (Waltham, US)
Freezer -80°C Hera Freeze HFU	Thermo Scientific (Waltham, US)
Fusion Fx7	Vilber (Eberhardzell, GER)
Incubator Heraeus HERAcell	Kendro Lab. Prod. (Hanau, GER)
Incubator HeraTherm	Thermo Scientific (Waltham, US)

Magnetic stirrer IKA KMO2 basic	IKA (Staufen, GER)
Magnetic stirrer IKA RCT basic	IKA (Staufen, GER)
Microscope Axio Imager.M2	Zeiss (Oberkochen, GER)
Microscope Observer.Z1	Zeiss (Oberkochen, GER)
Microscope Wilovert 30	Helmut Hund (Wetzlar, GER)
Millipore Q-Pod	Merck (Darmstadt, GER)
NanoDrop ND-1000	PEQLAB (Erlangen, GER)
pH-meter Lab850	SI Analytics (Mainz, GER)
Pipette Multichannel 100µl	Eppendorf (Hamburg, GER)
Pipettes 2µl, 10µl, 20µl, 100µl, 200µl, 1000µl	Gilson (Middleton, US)
pipetus-akku	Hirschmann (Eberstadt, GER)
Refrigerator	Siemens (München, GER)
Scale Acculab ALC 3100.2	Sartorius (Göttingen, GER)
Shaker Miniature M2	Edmund Bühler (Hechingen, GER)
Shaker ST5	CAT (Ballrechten-Dott., GER)
Vacuum pump	Vacuubrand (Wertheim, GER)
Vortex-Genie 2	Scientific Ind. (Bohemia, US)
Water bath	Memmert (Schwabach, GER)
Water bath GFL 1005	GFL (Burgwedel, GER)

2.2 Consumables

Table 4: List of used consumables

Consumables	Company
10cm/15cm culture plate	Thermo Scientific (Waltham, US)
6/12-well tissue culture plate	Corning (New York, US)
96-well plate, MaxiSorp	Thermo Scientific (Waltham, US)
Blotting paper, PVDF, 0.2µm	BIO-RAD (Hercules, US)
Chamber slide, 8 well	Thermo Scientific (Waltham, US)
Cell scraper	Falcon (Mexico City, Mexico)
Cell strainer (30µm, 70µm)	Falcon (Mexico City, Mexico)
Coverslips	Thermo Scientific (Waltham, US)
EDTA S-Monovette	Sarstedt (Nürnbrecht, GER)
FACS tubes	BD Falcon (Franklin Lakes, US)
Filter paper: Extra thick blot paper	BIO-RAD (Hercules, US)
Filter tips (0,1-10µl, 20µl, 200µl, 1000µl)	PEQLAB (Erlangen, GER)
Gloves	B. Braun (Melsungen, GER)
Microscope slides Superfrost Plus	Thermo Scientific (Waltham, US)
Millex-GV, 0.22µm, PVDF	Merck Millipore (Darmstadt, GER)
Parafilm M	Bemis (Neenah, US)
Pipet tips (with micropillary for loading gels)	VWR (Radnor, US)
Pipette tips TipOne (10-20µl, 200µl, 1000µl)	Starlab (Hamburg, GER)
Safe lock tubes (0.5ml, 1.5ml, 2ml)	Eppendorf (Hamburg, GER)
Serological pipettes (5ml, 10ml, 20ml)	Costar (Richmond, US)
Surgipath DB80 LS Premium Blades	Leica (Wetzlar, GER)
Syringes (1ml, 5ml, 10ml)	B. Braun (Melsungen, GER)
Falcon Tubes (15ml, 50ml)	Corning (New York, US)

2.3 Assay Kits

Table 5: List of used assay kits

Assay Kits	Company
Duoset ELISA Kit, human CCL2 IL-1β IL-6 IL-8 TNF-α	R&D Systems (Minneapolis, US)
DuoSet ELISA Kit, mouse Ccl2 Cxcl1 Icam-1 Il-1β Il-6 Tnf-α	R&D Systems (Minneapolis, US)
ELISA Kit, mouse Ccl5 Cxcl16 Il-1β Il-6	Invitrogen (Carlsbad, US)
Monocyte Isolation Kit, human	Miltenyi Biotec (Bergisch Gladbach, GER)
Omniscript RT Kit	Qiagen (Venlo, Netherlands)
RNA Isolation Kit: RNeasy Mini Kit	Qiagen (Venlo, Netherlands)

2.4 Chemicals and Reagents

Table 6: List of used chemicals and reagents

Chemicals and Reagents	**Company**
Acrylamid 30%	Serva (Heidelberg, GER)
APS	Thermo Scientific (Waltham, US)

BSA	Sigma (St. Louis, US)
Dimethyl Sulfoxid (DMSO)	Sigma (St. Louis, US)
Dithiothreitol	Thermo Scientific (Waltham, US)
Ethylenediamine-tetraacetic acid (EDTA)	Sigma (St. Louis, US)
Ethanol 70%	Institute-own
FACS staining buffer	Invitrogen (Carlsbad, US)
Ficoll-Paque Plus	GE Healthcare (Little Chalfont, UK)
Gentamicin	Thermo Scientific (Waltham, US)
Glycin	Merck (Darmstadt, GER)
HBSS	Thermo Scientific (Waltham, US)
Immobilon Chemiluminescent HRP Substrate	Merck (Darmstadt, GER)
Isopropanole	Sigma (St. Louis, US)
Kaiser’s glycerol gelatine	Roth (Karlsruhe, GER)
LDS NuPage Sample Buffer 4x	Invitrogen (Carlsbad, US)
LPS	Sigma (St. Louis, US)
2-Mercaptoethanol	Thermo Scientific (Waltham, US)
Methanol >99%	Roth (Karlsruhe, GER)
Mounting solution (Aqua Polymount)	Sigma (St. Louis, US)
Novex Sharp restained protein standard	Invitrogen (Carlsbad, US)
Oil Red-O Solution	Sigma (St. Louis, US)
Paraformaldehyd 4% (PFA)	Morphisto (Frankfurt M, GER)
Phosphatase Inhibitor	Roche (Basel, CH)
Propylene glycol	Sigma (St. Louis, US)
Protease Inhibitor	Roche (Basel, CH)
Restore Western Blot Stripping Buffer	Thermo S Scientific (Waltham, US)

RPMI 1640	Thermo Scientific (Waltham, US)
Sodium chloride	Roth (Karlsruhe, GER)
Sodium dodecyl sulfate (SDS)	Sigma (St. Louis, US)
TEMED	Roth (Karlsruhe, GER)
TissueTek O.C.T. Compound	Sakura (Alphen aan den Rijn, NL)
TMB Substrate Kit	Thermo Scientific (Waltham, US)
TMP195	Axon Medchem (Reston, US)
Recombinant Tnf-α	
human	Prepotech (Rocky Hill, US)
murine	Prepotech (Rocky Hill, US)
Triton X-100	Sigma (St. Louis, US)
Trizma Base	Sigma (St. Louis, US)
Trypanblue	Thermo Scientific (Waltham, US)
Tween 20	Roth (Karlsruhe, GER)

2.5 Antibodies for Immunoblot

Table 7: List of antibodies used for immunodetection

Antibody	Company	Dilution
Anti-IκBα	Cell Signaling	1:1000
Anti-p-IκBα	Cell Signaling	1:1000
Anti-p65	Santa Cruz	1:500
Anti-p-p65 (Ser 468)	Cell Signaling	1:1000
Anti-p-p65 (Ser536)	Cell Signaling	1:1000
Anti-β-Actin	Sigma Aldrich	1:5000
Anti-Tubulin	Sigma Aldrich	1:5000
Anti-rabbit IgG HRP	Dako	1:10000
Anti-mouse IgG HRP	Dako	1:10000

2.6 Buffers and solutions

2.6.1 Western Blot

Whole cell lysis buffer (12ml):

3 ml	4x LDS NuPage
1,5 ml	1M DTT
7,5 ml	ddH_2O
1	Phosphatase Inhibitor cocktail
1	Protease Inhibitor cocktail

Complete Lysis Buffer for Protein Concentration Measurement (50µl; for one culture plate):

5 µl	10mM DTT
44,5 µl	Lysis Buffer AM1
0,5 µl	Protease Inhibitor Cocktail

10% APS:

1g	APS 100%
	ad ddH_2O

Lower Tris 4x (pH=8,8):

90,85g (1,5M)	Tris Base
2g (0,4%)	SDS
	ad 0,5 l ddH_2O

Upper Tris 4x (pH=6,8):

30,3g (0,5M)	Tris Base
2g (0,4%)	SDS
	ad 0,5 l ddH_2O

Upper/Stacking Gel (for 2 gels with 1mm thickness):

2,9ml	ddH_2O
1ml	Upper Tris
0,6ml	Acrylamid 30%

45µl	APS 10%
4,5µl	TEMED

Lower/Running Gel 7,5% Acrylamid (for 2 gels with 1mm thickness):

5,9ml	ddH_2O
3ml	Lower Tris
3ml	Acrylamid 30%
100µl	APS 10%
10µl	TEMED

Lower Gel 10% Acrylamid (for 2 gels with 1mm thickness):

4,9ml	ddH_2O
3ml	Lower Tris
4ml	Acrylamid 30%
100µl	APS 10%
10µl	TEMED

TBS-T 10x:

500ml	1M Tris
438,3 g	NaCl
100ml	Tween20
	ad 5 l ddH_2O

TBS-T 1x:

100ml	TBS-t 10x
900ml	ddH_2O

Running Buffer 10x:

150 g (0,25M)	Tris Base
720 g (1,92M)	Glycin
50 g (1%)	SDS
	ad 5 l ddH_2O

Running Buffer 1x:

100ml	Running Buffer 10x
900ml	ddH_2O

Blotting Buffer 10x:

150 g	Tris Base
720 g	Glycin
	ad 5 l ddH_2O

Blotting Buffer 1x:

500 ml	Blotting Buffer 10x
1 L	Methanol
	ad 5 l ddH_2O

Blocking Buffer (1%):

5 g	BSA
500 ml	TBS-T 1x

Blocking Buffer (5%):

25 g	BSA
500 ml	TBS-T 1x

Stripping Buffer:

6,25 ml	1M Tris-HCl
20 ml	10% SDS
0,8 ml	β-Mercaptoethano

2.6.2 Cell culture

Phosphate buffer saline (PBS; 10x):

58,75 g	di-Sodium hydrogen phosphate
10 g	Monopotassium dihydrogen phosphate
400 g	Sodium chloride
10 g	Potassium chloride
	ad 5 l ddH_2O; pH 7,4

Basic monocytes medium:

500 ml	RPMI 1640 (+L-Glut)
50 ml	10% FCS
500 µl	Gentamicin

Bone marrow-derived macrophage growth medium (20ml):

17 ml	RPMI + FCS + Gentamycin
3 ml	L929-cell-conditioned medium (LCM)

FCS-free medium for stimulation:

500 ml	RPMI 1640 (+L-Glut)
500 µl	Gentamicin

2.6.3 Cell isolation

AUTOMACS Running Buffer:

25 g (0,5%)	BSA
3722 mg (2mM)	EDTA
4,5 g (0,09%)	Sodium azide NaN_3
500 ml	10x PBS
	ad 5 l dd H_2O

PBMC Isolation Buffer:

2 mM	EDTA
	In PBS pH 7,2

Monocyte Isolation Buffer:

2mM	EDTA
0,5 %	BSA
	in PBS pH 7,2

3 Methods

3.1 Mice and tissue harvesting

Hdac9$^{-/-}$ mice from E. Olson [72] were crossed with *Apoe*$^{-/-}$ mice for generation of *Hdac9*$^{-/-}$ *Apoe*$^{-/-}$ mice. Mice had access to ad libitum feeding and were housed in a specific pathogen-free animal facility with 12-hour light-dark cycles. Mice were fed either a chow diet or western-type diet (21%fat, 0.15% cholesterol) and were anesthetized using Medetomidine (0.5 mg/kg), Midazolam (5 mg/kg) and Fentanyl (0.05 mg/kg) or Ketamine-Xylazine. Blood was obtained through cardiac puncture and centrifuged for 10 min at 2000G for plasma collection in EDTA tubes. Thereafter, the arterial tree was perfused through the left ventricle using sterile 0.9% NaCl. The heart was removed and fixed in 4% paraformaldehyde (PFA) for sectioning and analysis of atherosclerotic plaques. Femur and tibiae were dissected from both legs and placed in sterile PBS for generation of bone marrow-derived macrophages (BMDMs) as described below.

3.2 Peritonitis model of acute inflammation

1 µg/ml of Lipopolysaccharide (LPS) was injected into the peritoneum of *Hdac9*$^{-/-}$ *Apoe*$^{-/-}$ and *Hdac9*$^{+/+}$ *Apoe*$^{-/-}$ mice for 24 hours. Mice were then sacrificed, and the peritoneal cavity was washed with 5 ml of ice-cold PBS + 1mM EDTA. The peritoneal exudate was obtained, and leukocyte influx was determined with hemocytometer counting. After centrifugation of the exudate, the supernatant was collected for analysis of cytokine production using ELISA. Peritoneal macrophages were obtained by adhesion to the tissue culture plate for 1 h and remaining cells washed five times with 1x PBS. Macrophages were then used for gene expression analysis by real time-PCR.

3.3 Cell culture

3.3.1 Generation of bone marrow-derived macrophages

Bone marrow-derived macrophages (BMDMs) were generated by flushing the bone marrow from femurs and tibiae of *Hdac9*$^{+/+}$ *Apoe*$^{-/-}$ and *Hdac9*$^{-/-}$ *Apoe*$^{-/-}$ mice with ice-cold PBS [109]. To create a single-cell suspension, cells were resuspended in PBS by repeated pipetting and filtered through a 40 µm cell strainer. Following centrifugation of the cell suspension at 500g for 10 min, the

pellet was resuspended in culture medium (RPMI 1640 containing 15% L929-cell-conditioned medium (LCM), 10% FCS and 100 µl/ml gentamycin) and plated on 15 cm untreated culture plates. 15% fresh LCM was added again on day 1 and 2 of culturing. After 7 days of culturing, differentiated macrophages were harvested by gentle scraping, and transferred onto untreated 6-well or 12-well plates for the stimulation experiments. Cells were left in LCM-free medium for 24 hours, giving them time to adhere. Cells were then stimulated in FCS-free medium with either 100 ng/ml LPS or 50 ng/ml Tnf-α for different time points.

3.3.2 Cell counting

Manual cell counting was performed using a hemocytometer with Neubauer counting grids. For this, 10 µl of Trypan blue were diluted in 90 µl of cell suspension. For automatic cell counting, cells were mixed with Trypan blue 1:1 and counted with an automated cell counter. Each sample was measured twice and the average taken as final cell number.

3.4 Western Blot

Cell lysis

After stimulation experiments, BMDMs were washed with ice-cold PBS and lysed with 100 µl/well NuPAGE-LDS buffer containing 1 mmol/l DTT and Phosphatase/Protease Inhibitor Cocktail for whole cell lysates.

Protein concentration measurement

Protein concentration was measured utilizing the Bradford Assay. A two-fold dilution series of BSA concentrations ranging from 20 µg/ml to 0 µl/ml was used for protein standard. For this, BSA was initially diluted in 1:50 Complete Lysis Buffer Dilution (10µl BSA in 990µl Complete Lysis Buffer Dilution for 20µl/ml). Samples were diluted 1:50 in ddH_2O. 25µl of each standard and sample was pipetted into a 96-well plate. Substrate A and B from the Bradford Assay Kit were mixed 1:50 and 200 µl of this mixed solution was added to each well. After incubation for 30 min at 37°C, samples were analyzed at 595nm wavelength using a spectrophotometer.

Sample preparation

Whole cell lysates were vortexed for 2 min and boiled at 95° C for 10 min. After centrifugation for 2 min at 11,000 rpm, samples were used for western blot analysis or stored at -20°C for later use.

SDS-PAGE Gel preparation

For 1 mm thick SDS-PAGE gels, upper and lower gel were prepared using the above-described volumes and chemicals. The lower gel solution was filled between two glass plates up to 80% level. Isopropanol was used to remove bubbles and ensure a straight surface, and washed off again with ddH_2O after 20 min, allowing the gel to polymerize. The upper gel solution and a 10-well or 15-well comb was added on top and again allowed to polymerize.

Protein electrophoresis

Gels were placed into an electrode chamber, and put into the electrophoresis tank with 1 x Running buffer. After careful removal of the combs, sample marker and samples were loaded into the wells of the SDS-PAGE gel with appropriate amounts of volume. Gels were run at a voltage of 120-150 V for 1 hour. SDS negatively charges the sample proteins, allowing negative proteins to migrate towards the positive electrode. Smaller proteins migrate faster than larger proteins. As a result, this procedure allows separation of proteins by molecular weight and length.

Transfer

To allow detection of proteins with antibodies, the proteins on the gel have to be transferred onto a PVDF membrane. For this, a 0.2 µm PVDF membrane has to be activated in methanol for 20-30 seconds and then placed into 1x Blotting Buffer together with filter paper and meshes. Using a defined order from cathode to anode (cathode – mesh – filter paper – gel – membrane – filter paper – mesh – anode), everything is placed into a transfer cassette that holds the gel in close contact with the membrane and placed in the blotting tank with 1x blotting buffer. For temperature control, an ice pack and magnetic stirrer were used as cooling mechanisms. Proteins are transferred for 1 hour at 100 V.

Immunodetection

After transfer, the membrane was blocked for 60 min at room temperature (RT) in 1% blocking buffer on shaker. Primary antibodies were incubated at 4°C overnight (anti-p-p65 S468 and S536, anti-IκBα, and anti-p- IκBα) or for 1 hour at room temperature (anti-Actin, anti-Tubulin and anti-P65) using above-described dilutions in 5% blocking buffer. Membranes were washed three times with 1x TBST for 5 minutes each on shaker. As secondary antibodies, HRP-conjugated anti-mouse or anti-rabbit antibodies were used for 1 hour at RT. After washing, blots were developed with Immobilon Western HRP Substrate by mixing Substrates 1:1 and visualized using the Fusion Fx7. If necessary, membranes were again washed after detection and stripped with stripping buffer for 10-15 min at RT on shaker for another different primary antibody. Quantification was performed using Image J 1.47v software.

3.5 ELISA

Measurements of cytokine and chemokine levels were performed using commercially available kits for Ccl2, Ccl5, Cxcl16, Cxcl1, Il1-β, Il-6 and Tnf-α as well as for IL-6, IL-8, IL1-β, CCL2 and TNF-α. For analysis of protein secretion in BMDMs and human monocytes, cells were stimulated with either 100 ng/ml LPS, 50 ng/ml mouse Tnf-α or human TNF-α as appropriate for indicated time points. Protein levels were measured in the supernatant using commercially available ELISA kits.

3.6 Quantitative Real-Time PCR

RNA was isolated from peritoneal macrophages using the RNeasy Mini Kit following the instructor's protocol and reverse-transcribed using oligo-dT (Table 8). RT-PCR analysis was performed using the SYBRgreen method with specific mouse primer pairs. Samples were run in duplicates or triplicates. *18S* was used as reference gene. Expression levels were determined by the comparative CT method (Fold change = $2^{\Delta\Delta C_T}$).

Table 8: List of used oligonucleotides

Gene (mouse)	Primer sequence
Ccl2 for	5'-CTTCTGGGCCTGCTGTTCA-3'
Ccl2 rev	5'-CCAGCCTACTCATTGGGATC-3'
Cxcl1 for	5'-TGC ACC CAA ACC GAA GTC AT-3'
Cxcl 1 rev	5'-TTG TCA GAA GCC AGC GTT CAC-3'
Il-1β for	5'-AGA GCA TCC AGC TTC AAA TCT C-3'
Il-1β rev	5'-CAG TTG TCT AAT GGG AAC GTC A-3'
Il-6 for	5'-TCA GGA AAT TTG CCT ATT GAA AA-3'
Il-6 rev	5'-CCA GCT TAT CTG TTA GGA GAG CA-3'
Tnf-α for	5'-ACC ACG CTC TTC TGT CTA CTG A-3'
Tnf-α for	5'-TCC ACT TGG TGG TTT GCT ACG-3'
18S	QuantiTect primer assay from Invitrogen

3.7 Study population and blood sampling

Patients were kindly recruited by Dr. Steffen Tiedt through the acute stroke unit of the Universitätsklinikum München (KUM) at Ludwig-Maximilians-University (LMU) in Munich, Germany in 2017. Candidates (n = 12) were selected based on ultrasound confirmed presence of atherosclerotic plaques in carotid artery or presence of carotid artery stenosis. Detailed demographic characteristics of the study population can be found in Table 9. Additionally, blood was collected from six young and healthy volunteers who are employees of KUM, LMU, Munich, Germany (age 25-51 years). 50 ml of whole blood was drawn into EDTA-plasma tubes and prepared for monocyte isolation. After approval by the local ethics committee, this study was conducted in accordance with the Declaration of Helsinki as well as institutional guidelines.

Table 9: Demographic characteristics and extracranial carotid duplex ultrasound findings of patients' blood used for monocyte isolation

Demographic characteristics	Statistics
Median age, years (IQR)	69.6 (17.4)
Female, n (%)	5 (41.7)
Vascular risk factors, n (%)	
Hypertension	11 (91.7)
Hypercholesterolemia	7 (58.3)
Diabetes	3 (25.0)
Current or past nicotine	3 (25.0)
Family history for CVD	1 (8.3)
Prior stroke/TIA	9 (75.0)
Extracranial carotid duplex scan, n (%)	12 (100.0)
Intima-Media thickness, mm (mean, SD)	0.94 (0.22)
Presence of plaques, n (%)	12 (100)

Abbreviations: Interquartile range (IQR), transient ischemic stroke (TIA), standard deviation (SD)

3.8 Isolation and treatment of human monocytes

Mononuclear cells from human peripheral blood were isolated by density gradient centrifugation. For this, 35 ml of diluted cell suspension (26 ml of isolation buffer added to 9 ml of whole blood) was carefully layered on 15 ml of Ficoll-Paque. After centrifugation for 30 min (400G, Acc 3, Decc 0) at RT, the mononuclear cell layer was transferred into a new conical tube. After several careful washing steps for removal of platelets, peripheral blood mononuclear cells (PBMCs) were prepared for magnetic labeling to isolate monocytes using the Monocyte Isolation Kit II following the manufacturer's protocol and the AutoMACS Pro Separator. For

this, non-monocytes are indirectly magnetically labeled using a cocktail of biotin-conjugated antibodies against Cd3, Cd7, Cd16, Cd19, Cd56, Cd123 and Glyophorin A and Anti-Biotin Microbeads and depleted by negative selection of unlabeled monocytes.

3.9 Pharmacological inhibition in diet-induced atherosclerosis

6-7 weeks old male *Apoe* $^{-/-}$ mice received daily intraperitoneal injections of 50µl vehicle DMSO or 50µl of the specific class IIa HDAC inhibitor TMP195 for four weeks while receiving a Western-type diet in parallel. Beforehand, to get the final concentration of 50mg/kg, TMP195 was dissolved in 100% DMSO.

3.10 Oil Red-O Staining and Atherosclerotic plaque analysis

After cardiac puncture and perfusion of the arterial tree through the left ventricle with 0,9% NaCl, the heart was removed and fixed in 4% paraformaldehyde (PFA). After briefly washing the heart in PBS, it was embedded in TissueTek for cryosectioning and staining. Hearts were cut with the Cryostat Leica CM1950 extending cranially with 5 µm thickness of each section. 5 different sections covering a total distance of 250-300 µm were selected for lipid staining using Oil Red-O. For this, slides were incubated in Oil Red-O Solution for 1 hour at 37°C. After several washing steps in propylene glycol and ddH_2O, slides were stained with hematoxylin for 30 seconds, followed by more washing. Sections were then quantified using the Software Image J and the average was taken to determine absolute lesion size as well as relative lesion size (lesion area divided by total area of aortic root). All experiments and data analysis were performed under blinded conditions for the genotypes.

3.11 Statistical Analysis

For statistical analysis, the software GraphPad Prism 6 (GraphPad Software Inc.) was used. All data are represented as means ± SEM. After testing for normality, data were analyzed by unpaired Student's t test with or without Welch's correction as appropriate or Mann–Whitney test, one-way or two-way ANOVA with Bonferroni or Holm-Sidak multiple comparison test or Kruskal-Wallis with Dunn's multiple comparison test, as appropriate. P values <0.05 were considered to be statistically significant.

4 Results

4.1 Hdac9 deficiency attenuates inflammation *in vivo*

The first aim of this project was to elucidate the mechanistic link between Hdac9 and inflammatory responses in atherosclerosis. For this, we employed mouse models of inflammation *in vivo* encompassing both acute and chronic inflammation.

4.1.1 Hdac9 deficiency reduces leukocyte recruitment and cytokine production in LPS-induced peritonitis model of acute inflammation

To investigate the effects of *Hdac9* deficiency in a setting of acute inflammation, we used the *in vivo* LPS peritonitis model. For this, *Hdac9*$^{-/-}$*Apoe*$^{-/-}$ mice and *Hdac9*$^{+/+}$*Apoe*$^{-/-}$ control littermates were intraperitoneally (i.p.) injected with LPS (1µg/ml) as a strong inducer of inflammation (Figure 7A). After 24 hours of stimulation, mice were sacrificed for quantification of leukocyte recruitment into the peritoneum using cell counting. The results showed significantly reduced cell numbers of leukocytes in the peritoneal exudate of *Hdac9*$^{-/-}$*Apoe*$^{-/-}$ mice (Figure 7B). Furthermore, the peritoneal exudate showed significantly reduced levels of the inflammatory cytokines Tnf-α and Cxcl1. However, the protein amounts of Il-6, Il1-β, Ccl2 and Ccl5 only showed trends of reduction without statistical significance (Figure 7C).

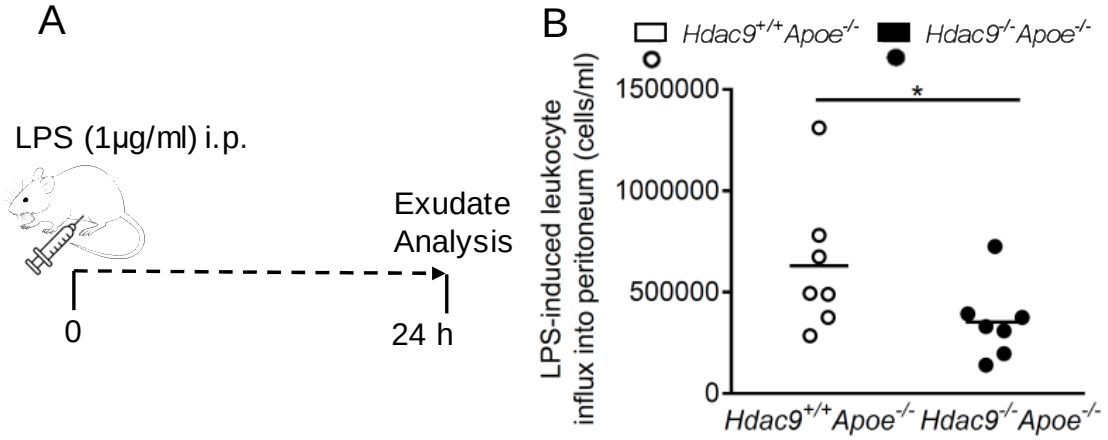

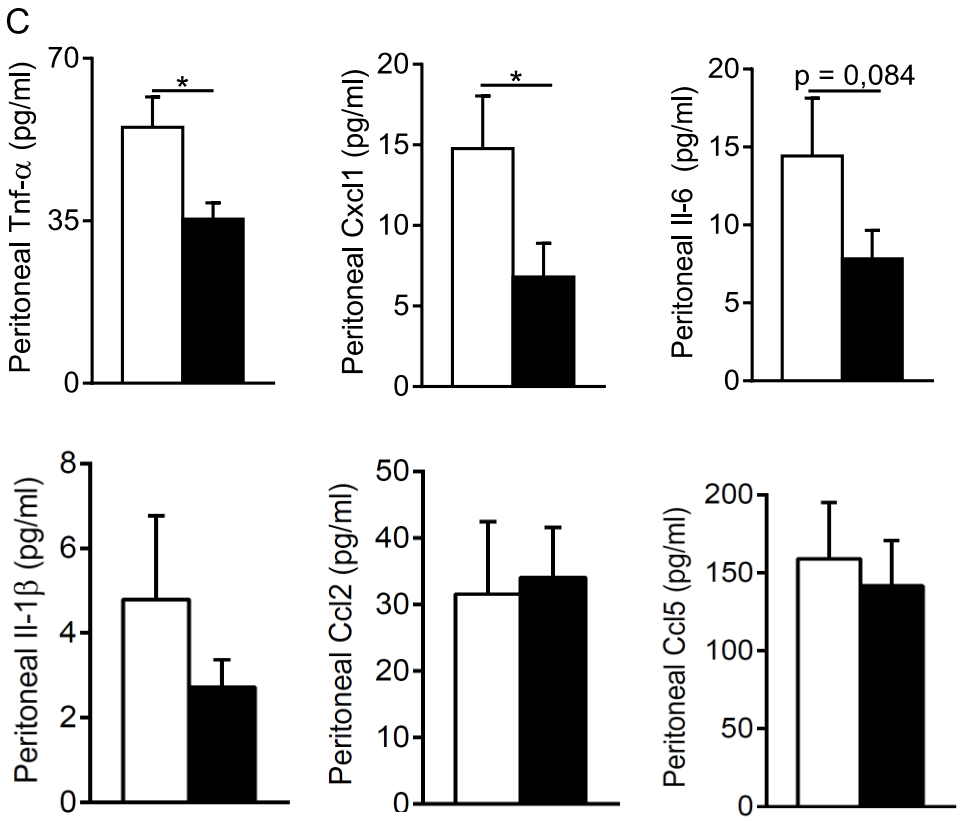

Figure 7. *Hdac9* deficiency reduces leukocyte recruitment and cytokine production in LPS-induced peritonitis model of acute inflammation

Experimental design for the LPS peritonitis model in (A): *Hdac9*$^{-/-}$*Apoe*$^{-/-}$ and *Hdac9*$^{+/+}$*Apoe*$^{-/-}$ control littermates received i.p. injections of LPS (1 µg/mL) for 24 h followed by analysis of exudates from the peritoneum. Number of recruited leukocytes into the peritoneum after 24 h of LPS stimulation was determined (B). Peritoneal protein levels of pro-inflammatory cytokines with 5-9 mice per group were analyzed using ELISA (C). Data represent means ± SEM. Unpaired t-test or Mann-Whitney test, as appropriate, for comparison of *Hdac9*$^{-/-}$*Apoe*$^{-/-}$ vs. *Hdac9*$^{+/+}$*Apoe*$^{-/-}$: *, $p<0.05$; **, $p<0.01$.

4.1.2 Hdac9 deficiency reduces levels of circulating Cxcl1 in a chronic inflammation model of spontaneous atherosclerosis

To test the effects of *Hdac9* deficiency under chronic atherogenic conditions, an inflammation model of spontaneous atherosclerosis was employed in *Hdac9*$^{-/-}$*Apoe*$^{-/-}$ mice and *Hdac9*$^{+/+}$*Apoe*$^{-/-}$ control littermates. Mice were fed a standard chow diet and sacrificed at either 18 weeks or 28 weeks of age (Figure 8A). For both groups, serum was obtained by cardiac puncture. ELISA measurements revealed significantly reduced levels of circulating Cxcl1 in 28 weeks *Hdac9*$^{-/-}$*Apoe*$^{-/-}$ old mice compared to *Hdac9*$^{+/+}$*Apoe*$^{-/-}$ (Figure 8C). In

contrast, in 18 weeks old *Hdac9*$^{-/-}$ *Apoe*$^{-/-}$ mice, Cxcl1 levels did not show any significant difference to their control littermates (Figure 8B).

Taken together, these findings demonstrate that HDAC9 promotes both acute and chronic inflammation *in vivo*.

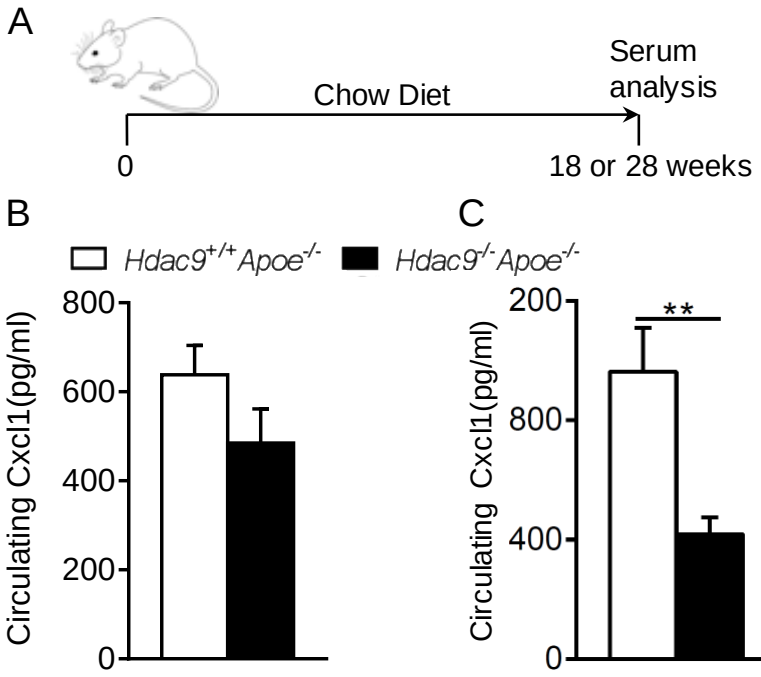

Figure 8. *Hdac9* deficiency reduces levels of circulating Cxcl1 in a chronic inflammation model of spontaneous atherosclerosis

Experimental design for mice model of chronic inflammation in (A): *Hdac9*$^{-/-}$*Apoe*$^{-/-}$ and *Hdac9*$^{+/+}$*Apoe*$^{-/-}$ control littermates were fed a chow diet for 18 and 28 weeks. Serum was obtained for protein analysis using ELISA. Quantifications of 9-12 mice per group for 18 weeks (B) and 15-19 mice per group for 28 weeks (C) with mixed male and female gender. Data represent means ± SEM. Unpaired t-test for comparison of *Hdac9*$^{-/-}$*Apoe*$^{-/-}$ vs. *Hdac9*$^{+/+}$*Apoe*$^{-/-}$: *, $p<0.05$; **, $p<0.01$.

4.2 Hdac9 deficiency limits pro-inflammatory responses in macrophages *in vitro* and *in vivo*

The previously described findings strongly suggest that HDAC9 promotes inflammation. To further study the role of Hdac9 in specific cell-types involved in vascular inflammation, we decided to focus on monocytes and macrophages, as they are known to play crucial roles in atherogenesis. More specifically, we investigated the effects of *Hdac9* deficiency on inflammation in murine bone marrow-derived macrophages (BMDMs) *in vitro* and in peritoneal macrophages *in vivo*.

4.2.1 Hdac9 deficiency reduces cytokine and chemokine secretion in LPS- and Tnf-α stimulated BMDMs in vitro

For this analysis, BMDMs from *Hdac9*$^{-/-}$*Apoe*$^{-/-}$ mice and *Hdac9*$^{+/+}$*Apoe*$^{-/-}$ control littermates were stimulated with LPS (100 ng/ml) for 24 hours to check inflammation-triggered cytokine and chemokine secretion. Protein analysis revealed significantly reduced levels of the pro-inflammatory cytokines and chemokines Tnf-α, Cxcl1, Il1-β, Ccl2 and Il-6 in *Hdac9*- and *Apoe*-deficient macrophages compared to just *Apoe*-deficient mice (Figure 9 A-E). This clearly suggests that HDAC9 limits pro-inflammatory responses in macrophages *in vitro*.

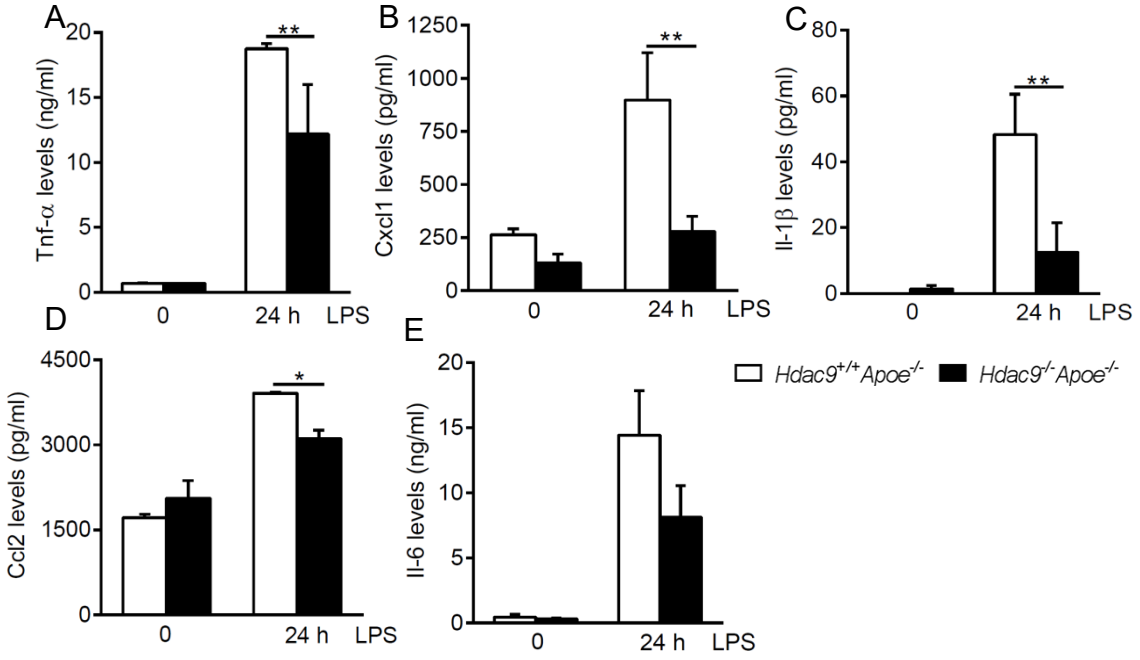

Figure 9. *Hdac9* deficiency reduces cytokine and chemokine secretion in LPS-stimulated BMDMs *in vitro*

BMDMs were generated from *Hdac9*$^{-/-}$*Apoe*$^{-/-}$ and *Hdac9*$^{+/+}$*Apoe*$^{-/-}$ control mice and stimulated with LPS (100ng/ml) for 24 h or left untreated as indicated. Supernatant was collected and pro-inflammatory cytokine levels for Tnf-α (A), Cxcl1 (B), Il1-β (C), Ccl2 (D) and Il-6 (E) were determined using ELISA. Quantifications show n = 5 mice per group. Data represents means ± SEM. Two-way ANOVA with Bonferroni post-test for comparison of *Hdac9*$^{-/-}$ Apoe$^{-/-}$ vs. Hdac9$^{+/+}$Apoe$^{-/-}$: *, p<0.05; **, p<0.01.

Tnf-α acts as a more endogenous inflammatory and atherosclerosis relevant stimulus, hence mimicking a more physiological setting of inflammation. We therefore analyzed pro-inflammatory responses in BMDMs stimulated with 50 ng/ml Tnf-α for 24 hours. Levels of Tnf-α, Cxcl1, Il1-β and Ccl2 were significantly reduced (Figure 10 A-D), while leaving Il-6 unaffected (Figure 10E).

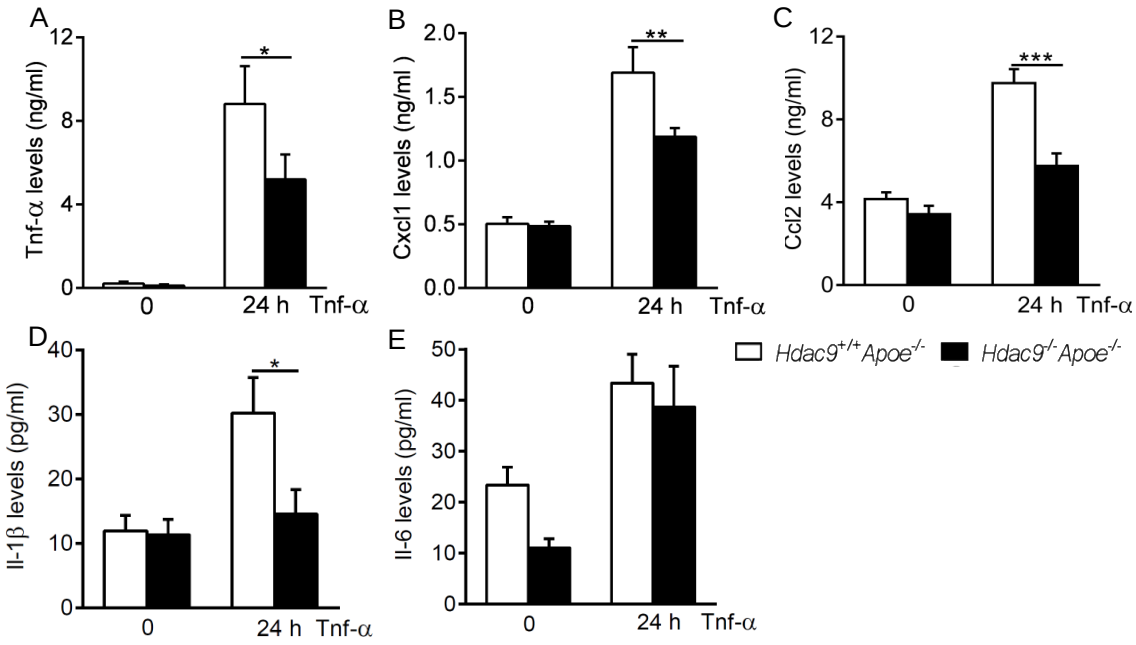

Figure 10. *Hdac9* deficiency reduces cytokine and chemokine secretion in Tnf-α stimulated BMDMs *in vitro*

BMDMs were generated from *Hdac9*$^{-/-}$*Apoe*$^{-/-}$ and *Hdac9*$^{+/+}$*Apoe*$^{-/-}$ control mice and stimulated with mTnf-α (50ng/ml) for 24 h or left untreated as indicated. Supernatant was collected and pro-inflammatory cytokine levels for Tnf-α (A), Cxcl1 (B), Ccl2 (C), Il1-β (D) and Il-6 (E) were determined using ELISA. Quantifications show n = 6-10 mice per group. Data represents means ± SEM. Two-way ANOVA with Bonferroni post-test for comparison of *Hdac9*$^{-/-}$*Apoe*$^{-/-}$ vs. *Hdac9*$^{+/+}$*Apoe*$^{-/-}$*:* *, p<0.05; **, p<0.01; ***, p<0.001

4.2.2 Hdac9 deficiency reduces pro-inflammatory gene expression of LPS-stimulated peritoneal macrophages in vivo

To investigate whether these *in vitro* findings in LPS- and Tnf-stimulated macrophages can be recapitulated *in vivo*, we studied the effects of *Hdac9* deficiency on macrophage function and gene transcription using the previously described LPS peritonitis model *in vivo*. *Hdac9*$^{-/-}$*Apoe*$^{-/-}$ mice and *Hdac9*$^{+/+}$*Apoe*$^{-/-}$ mice received intraperitoneal injections of LPS for 24 hours. After stimulation, peritoneal macrophages were isolated and analyzed for pro-inflammatory gene expression (Figure 11A). The results showed a significant downregulation of the genes *Cxcl1, Il1-β, Il-6* and a trend for *Tnf-α* and *Ccl2* in the *Hdac9*-deficient mice (Figure 11B). Together, this corroborates the pro-inflammatory role of Hdac9 in macrophages *in vivo.*

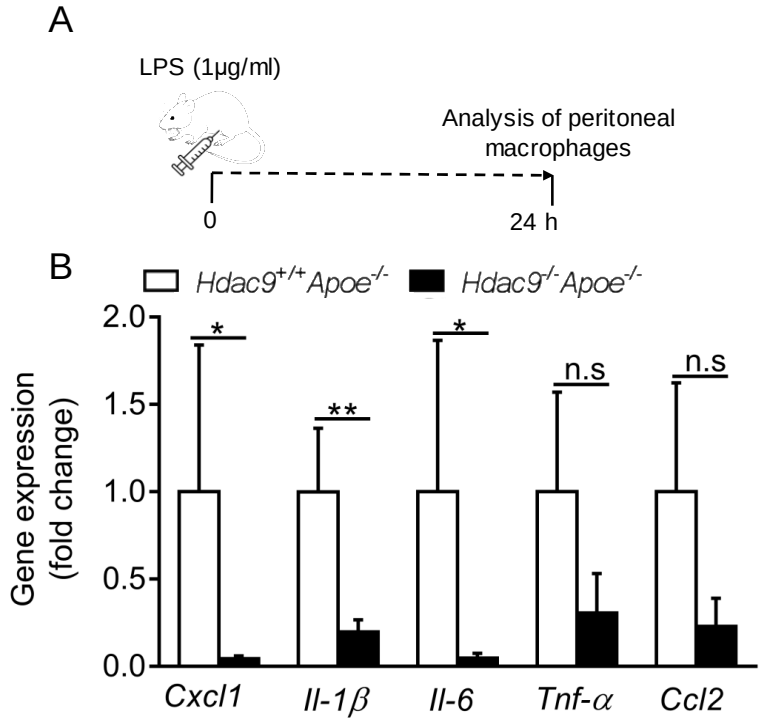

Figure 11. *Hdac9* deficiency reduces pro-inflammatory gene expression of LPS-stimulated peritoneal macrophages *in vivo.*

Experimental design in (A): *Hdac9*$^{-/-}$*Apoe*$^{-/-}$ and *Hdac9*$^{+/+}$*Apoe*$^{-/-}$ control littermates were injected i.p. with LPS (1 µg/mL) for 24 h, followed by analysis of peritoneal macrophages. Pro-inflammatory genes were quantified and normalized to *18S* with 7-9 mice in a group (B). Data represent means ± SEM. Mann-Whitney test for comparison of *Hdac9*$^{-/-}$*Apoe*$^{-/-}$ vs. *Hdac9*$^{+/+}$*Apoe*$^{-/-}$*:* *, p<0.05; **, p<0.01; ***, p<0.001; ****, p<0.0001.

In summary, these data suggest that Hdac9 has a pro-inflammatory effect on cytokine production in macrophages with a stimulus-dependent pattern of affected cytokines.

4.3 Hdac9 enhances p65 phosphorylation at serine residues 536 and 468

As reviewed in Chapter 1.4, NF-κB is a master regulator of inflammation [83]. Many of the atherosclerosis-relevant inflammatory chemokines and cytokines that we found to be affected by Hdac9 are also targets of the NF-κB pathway. Thus, we examined the effects of *Hdac9* deficiency on NF-κB signaling. More specifically, we focused on the phosphorylation status of p65 since this form of PTM is known to be essential for function and regulation of NF-κB transcriptional activity [84]. We analyzed the phosphorylation status of two different serine residues – S536 and S468 in BMDMs, both located in the transactivation domain of p65, by Western blotting using antibodies recognizing the phosphorylated p65 (located at ~65kDa).

4.3.1 Hdac9 deficiency reduces p65 phosphorylation in LPS- and Tnf-α stimulated BMDMs

After stimulation of BMDMs for the time frame of 0, 5, 15 or 45 minutes with 100 ng/ml LPS, no significant difference of the phosphorylation status at both S536 (Figure 12 A, B) and S468 (Figure 12 C, D) could be detected when comparing *Hdac9*-deficient BMDMs to controls. To examine possible effects of *Hdac9* deficiency on p65 phosphorylation after longer periods of LPS exposure, we again stimulated BMDMs with 100 ng/ml, but in this experiment for 0.5, 1.5, 2, 4 and 6 hours. This time, results showed significantly reduced phosphorylation of p65 at S536 after 6 h (Figure 12 E, F) and for S468 after 0.5 h of LPS stimulation (Figure 12 G, H).

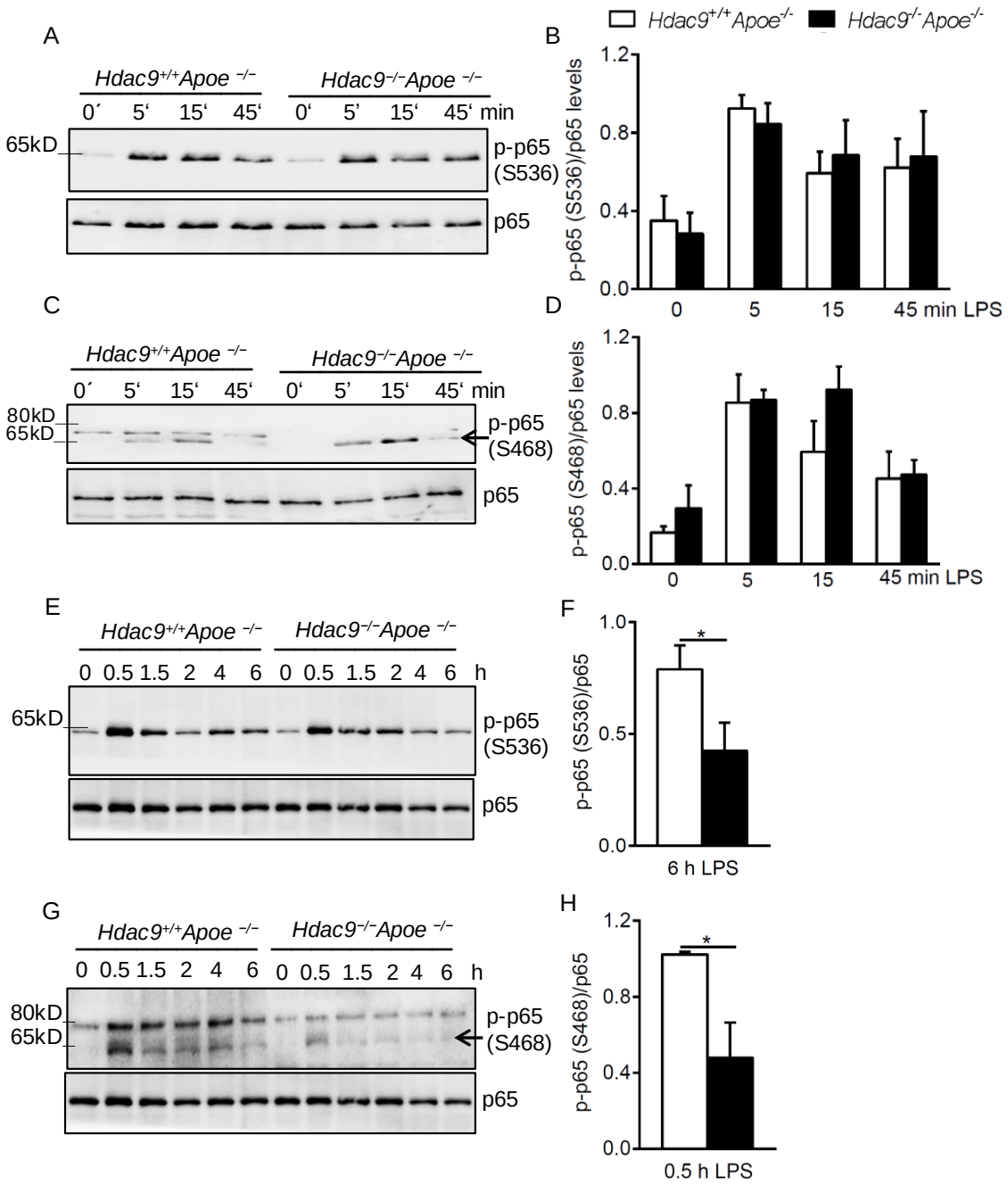

Figure 12. *Hdac9* deficiency reduces p65 phosphorylation at S536 and S468 in LPS-stimulated BMDMs

BMDMs were generated from *Hdac9*$^{-/-}$*Apoe*$^{-/-}$ and *Hdac9*$^{+/+}$*Apoe*$^{-/-}$ control mice after which cells were stimulated with LPS (100 ng/mL) for shorter time periods of 5, 15 and 45 min (A-D) or longer time periods of 0.5, 1.5, 2, 4 and 6 h (E-H). Shown in (A, E) for S536 and (C, G) for S468 are representative immunoblots of p-p65 (65kDa) and p65 (65kDa) as loading control. Phosphorylation of p65 at S536 and S468 was quantified after normalization to total p65 with n = 5 mice in a group. Data represents means ± SEM. Two-way ANOVA with Bonferroni post-test for comparison of *Hdac9*$^{-/-}$*Apoe*$^{-/-}$ vs. *Hdac9*$^{+/+}$*Apoe*$^{-/-}$ control: *, $p<0.05$.

In the same experimental setting, but stimulating with the more endogenous inflammation trigger Tnf-α for 0, 5, 15 and 45 min, immunoblots showed significantly reduced phosphorylation of p65 at S536 after 45 min (Figure 13 A, B). Similar results were obtained for the second serine residue of interest, S468. Here, the significant effect can be found after 5 min of Tnf-α stimulation in the *Hdac9*-deficient macrophages (Figure 13 C, D).

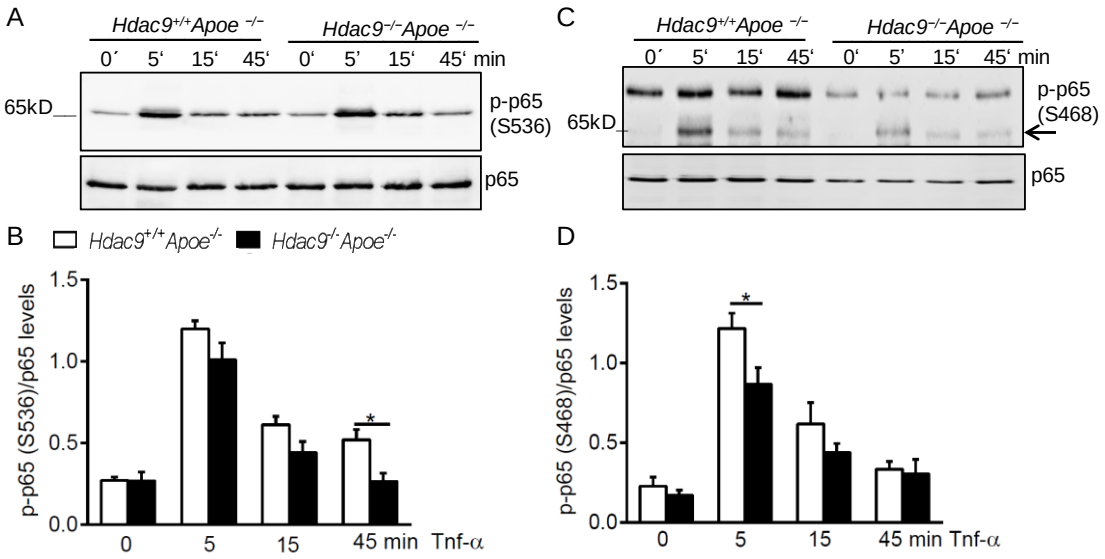

Figure 13. Hdac9 deficiency reduces p65 phosphorylation at S536 and S468 in Tnf-α stimulated BMDMs

BMDMs were generated from *Hdac9*$^{-/-}$*Apoe*$^{-/-}$ and *Hdac9*$^{+/+}$*Apoe*$^{-/-}$ control mice after which cells were stimulated with mTnf-α (50 ng/mL) for 5, 15 and 45 min or left untreated. Shown in (A) are representative immunoblots of p-p65 S536 (65kDa) and p65 (65kDa) as loading control. Phosphorylation of p65 at S536 was quantified after normalization to total p65 in (B) with n = 8 mice in a group. Shown in (C) are representative immunoblots of p-p65 S468 (65kDa) and p65 (65kDa) as loading control. Phosphorylation of p65 at S468 was quantified after normalization to total p65 in (D) with n = 5 mice in a group. Data represents means ± SEM. Two-way ANOVA with Bonferroni post-test for comparison of *Hdac9*$^{-/-}$*Apoe*$^{-/-}$ vs. *Hdac9*$^{+/+}$*Apoe*$^{-/-}$: *, $p<0.05$.

Collectively, the results indicate that HDAC9 is required for sustained p65 phosphorylation at both serine residues S536 and S468.

4.4 Hdac9 enhances de novo synthesis of IκB-α in pro-inflammatory macrophages

NF-κB promotes de novo synthesis of the inhibitory protein IκB-α as part of a regulatory negative feedback loop. Therefore, we quantified IκB-α levels in BMDMs derived from *Hdac9*$^{-/-}$*Apoe*$^{-/-}$ mice and *Hdac9*$^{+/+}$*Apoe*$^{-/-}$ mice as a possibility to further study transcriptional NF-κB activity in *Hdac9*-deficient macrophages.

4.4.1 Hdac9 deficiency reduces de novo synthesis of IκB-α in LPS- and Tnf-α stimulated BMDMs without affecting its proteasomal degradation

First, we generated BMDMs from *Hdac9*$^{-/-}$*Apoe*$^{-/-}$ mice and *Hdac9*$^{+/+}$*Apoe*$^{-/-}$ mice and stimulated the cells with 100 ng/ml LPS for 5, 15, 45 min or left them untreated. Western blot analysis of IκB-α (39 kDa) did not show any significant results for any of these time points (Figure 14 A, B). Since our previous results suggested prolonged LPS-mediated inflammatory effects, we extended the stimulation times of the experiment. BMDMs were again stimulated for 0.5, 1.5, 2, 4 and 6 hours. This time, significant reduction of IκB-α could be found after 90 min of stimulation in *Hdac9*-deficient macrophages (Figure 14 C, D).

Phosphorylation of IκB-α marks it for proteasomal degradation. Thus, to investigate whether HDAC9 has effects on IκB-α degradation, we again stimulated BMDMs with LPS for the same time points as before and analyzed levels of phosphorylated IκB-α (40 kDa). No difference between *Hdac9*-deficient and control macrophages could be detected (Figure 14 A, B). Therefore, proteasomal degradation of IκB-α is not affected by Hdac9.

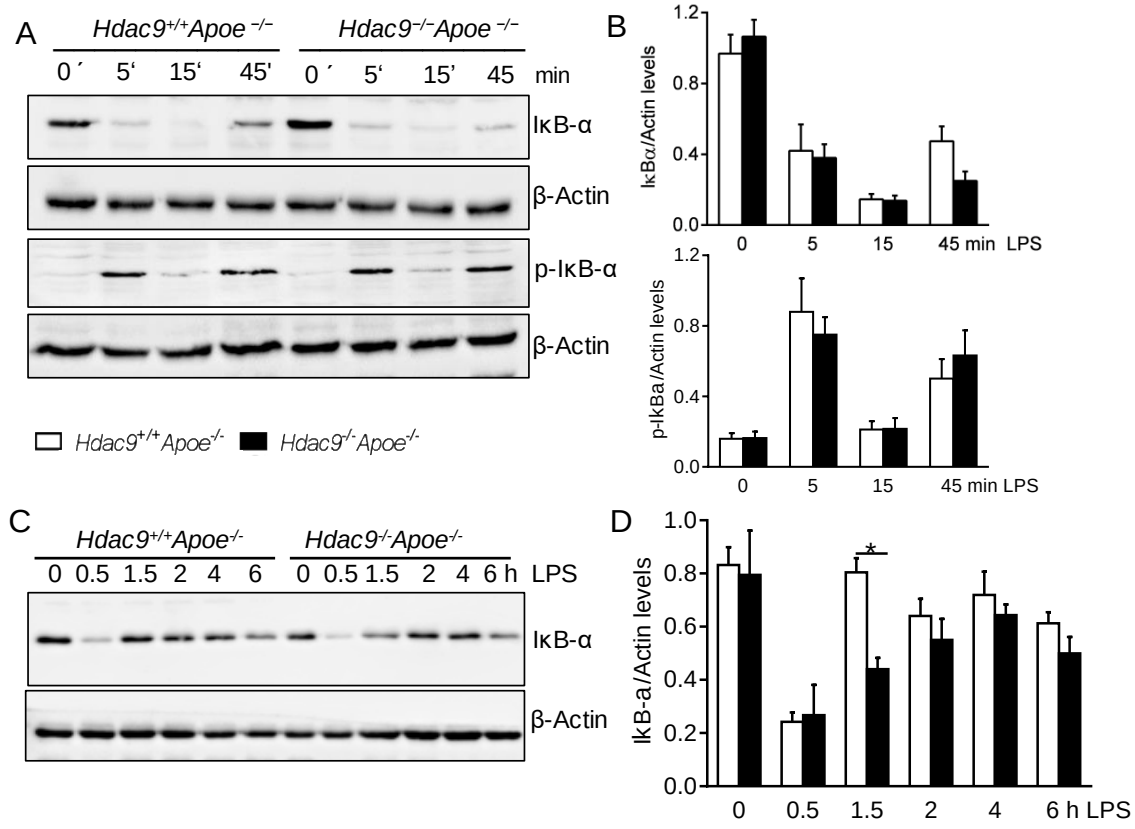

Figure 14. *Hdac9* deficiency reduces de novo synthesis of IκB-α in LPS-stimulated BMDMs.

BMDMs were generated from *Hdac9*$^{-/-}$*Apoe*$^{-/-}$ and *Hdac9*$^{+/+}$*Apoe*$^{-/-}$ control mice after which cells were stimulated with LPS (100 ng/mL) for 5, 15 and 45 min or left untreated (A, B). Shown in (A) are representative immunoblots of IκB-α (39 kDa) and p-IκB-α (40 kDa) with β-Actin (42 kDa) as loading control. Protein levels of IκB-α and p-IκB-α (B) were quantified after normalization to total β-actin (n = 8 mice per group). For longer timepoints, cells were stimulated for 0.5, 1.5, 2, 4 and 6 hours or left untreated. Shown in (C) are representative immunoblots of IκB-α (39kDa) with β-Actin (42kDa) as loading control. Protein levels of IκB-α at all timepoints (D) were quantified after normalization to total β-Actin (n = 3 mice per group). Data represents means ± SEM. Two-way ANOVA with Bonferroni post-test or Mann-Whitney test for comparison *Hdac9*$^{-/-}$*Apoe*$^{-/-}$ vs. *Hdac9*$^{+/+}$*Apoe*$^{-/-}$ control*:* *, $p<0.05$.

Again, using the endogenous stimulus Tnf-α in the same experimental setup as before, BMDMs were stimulated with 50ng/ml Tnf-α. Western blot analysis revealed reduced protein levels of IκB-α after 45 minutes of stimulation in *Hdac9*-deficient macrophages (Figure 15 A, B). For p-IκB-α, quantification showed no significant difference in *Hdac9*-deficient macrophages compared to their control littermates (Figure 15 A, C).

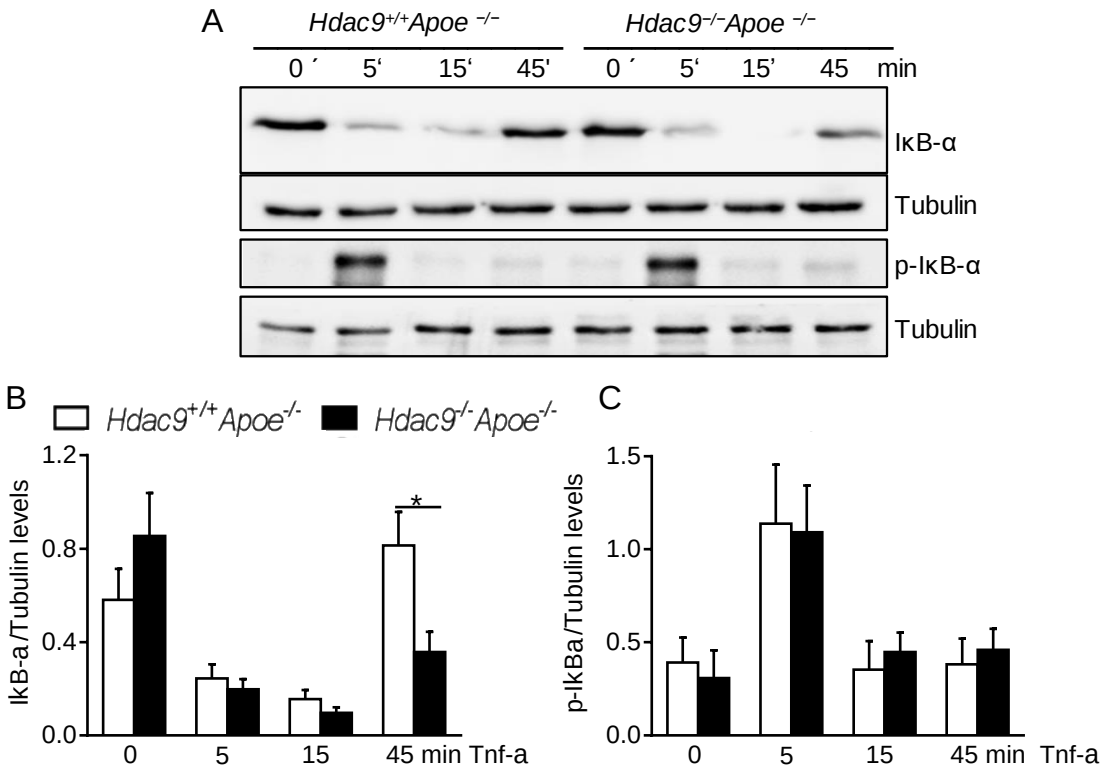

Figure 15. *Hdac9* deficiency reduces *de novo* synthesis of IκB-α in Tnf-α stimulated BMDMs.

BMDMs were generated from *Hdac9*$^{-/-}$*Apoe*$^{-/-}$ and *Hdac9*$^{+/+}$*Apoe*$^{-/-}$ control mice after which cells were stimulated with Tnf-α (50 ng/mL) for 5, 15 and 45 min or left untreated. Shown in (A) are representative immunoblots of IκB-α (39kDa) and p-IκB-α (40kDa) with Tubulin (50kDa) as loading control. Protein levels of IκB-α (B) or p-IκB-α (C) was quantified after normalization to total Tubulin with n = 8 mice in a group. Data represents means ± SEM. Two-way ANOVA with Bonferroni post-test for comparison of *Hdac9*$^{-/-}$*Apoe*$^{-/-}$ vs. *Hdac9*$^{+/+}$*Apoe*$^{-/-}$ control*:* *, $p<0.05$.

Overall, these data demonstrate that Hdac9 enhances IκB-α *de novo* synthesis for both Tnf-α- and LPS-stimulated macrophages at different time points without affecting phosphorylation of IκB-α.

4.5 Selective pharmacological inhibition of class IIa HDACs has atheroprotective and anti-inflammatory effects in *Apoe*$^{-/-}$ mice

A highly selective class IIa HDAC inhibitor TMP195 has been successfully used in mice with less cytotoxicity and significant anti-tumorigenic effects [81]. Thus, TMP195 provided a great opportunity for this study to explore the effects of selective class IIa HDAC inhibition on inflammation and atherosclerosis *in vivo* as well as *in vitro.*

4.5.1 TMP195 treatment of Tnf-α-stimulated BMDMs reduces pro-inflammatory cytokine production in vitro

Given the indicated anti-inflammatory effect of *Hdac9* deficiency in BMDMs as demonstrated above, we assessed whether similar effects can be found in *Apoe*-deficient BMDMs treated with TMP195. BMDMs were generated from *Apoe*$^{-/-}$ mice and incubated with different concentrations of TMP195 (0.5, 1, 3 and 5 µM) for one hour. Subsequently, cells were stimulated with Tnf-α for 24 h and supernatant was used for ELISA analysis of pro-inflammatory cytokines and chemokines. Here, we found significantly reduced protein levels for Il-6 in cells treated with 5 µM TMP195 (Figure 16A). The remaining cytokines and chemokines Il1-β, Ccl2, Cxcl1 and Tnf-α did not show any statistically significant effects, but showed a clear trend of reduction with increasing concentrations of the inhibitor (Figure 16 B-E).

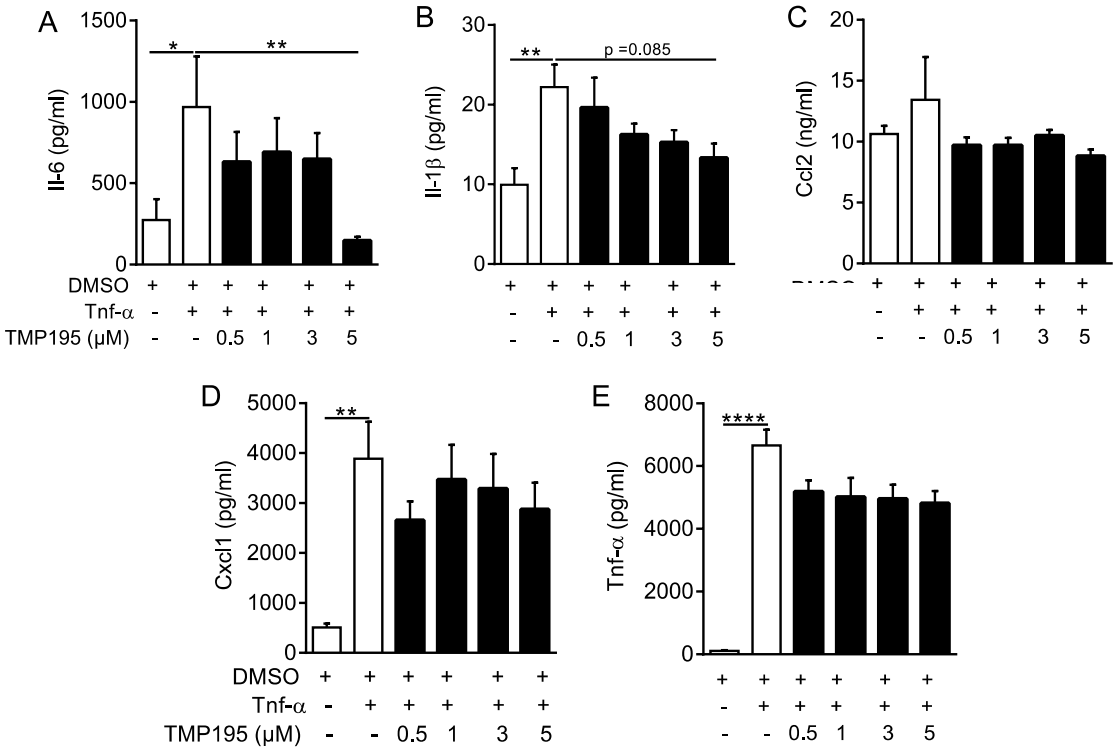

Figure 16. TMP195 treatment of Tnf-α stimulated BMDMs reduces inflammatory cytokine production *in vitro*.

BMDMs were generated from *Apoe*$^{-/-}$ mice and pretreated with different concentrations of TMP195 (0.5, 1, 3 or 5 µM) or DMSO (vehicle) for 1 h and either stimulated with Tnf-α (50 ng/mL) for 24 h or left untreated. Supernatants were collected at the end of stimulation and cytokine levels were analysed using ELISA for n = 9 mice per group (A-E). Data represent means ± SEM. One-way

ANOVA with Holm-Sidak multiple comparison test or Kruskal-Wallis with Dunn's multiple comparison test, as appropriate, for comparison of TMP195 vs. Vehicle control: *, p<0.05; **, p<0.01; ***, p<0.001; ****, p<0.0001

4.5.2 TMP195 treatment of Tnf-α stimulated BMDMs reduces p65 phosphorylation at serine residue 536

As described earlier, our experiments showed altered NF-κB signaling in *Hdac9*-deficient BMDMs (Subchapter 4.3 and 4.4). Hence, we examined the effects of TMP195 treatment on NF-κB signaling by analyzing the effects on phosphorylation of p65 at S536 and S468 in Tnf-α-stimulated BMDMs when incubated with different concentrations of the inhibitor beforehand.

First, we analyzed p65 phosphorylation at S536. For this purpose, BMDMs were generated from *Apoe*$^{-/-}$ mice and pretreated with 0.5, 1 or 3 µM of TMP195 for one hour. Cells were then stimulated with Tnf-α for 5 or 45min and supernatant was used for Western Blot analysis of p-p65 S536 (65kDa). For 5 min of stimulation, increasing concentrations of the inhibitor resulted in significant reduction of p-p65 protein levels (Figure 17 A, B). BMDMs stimulated for 45 min on the other hand did not show any significant changes (Figure 17 C, D). Next, p65 phosphorylation of S468 in TMP195-treated BMDMs was analyzed with the same experimental design as described before. This time, TMP195 did not significantly affect S468 p65 phosphorylation for either 5 min or 45 min of Tnf-α stimulation (Figure 17 E- H).

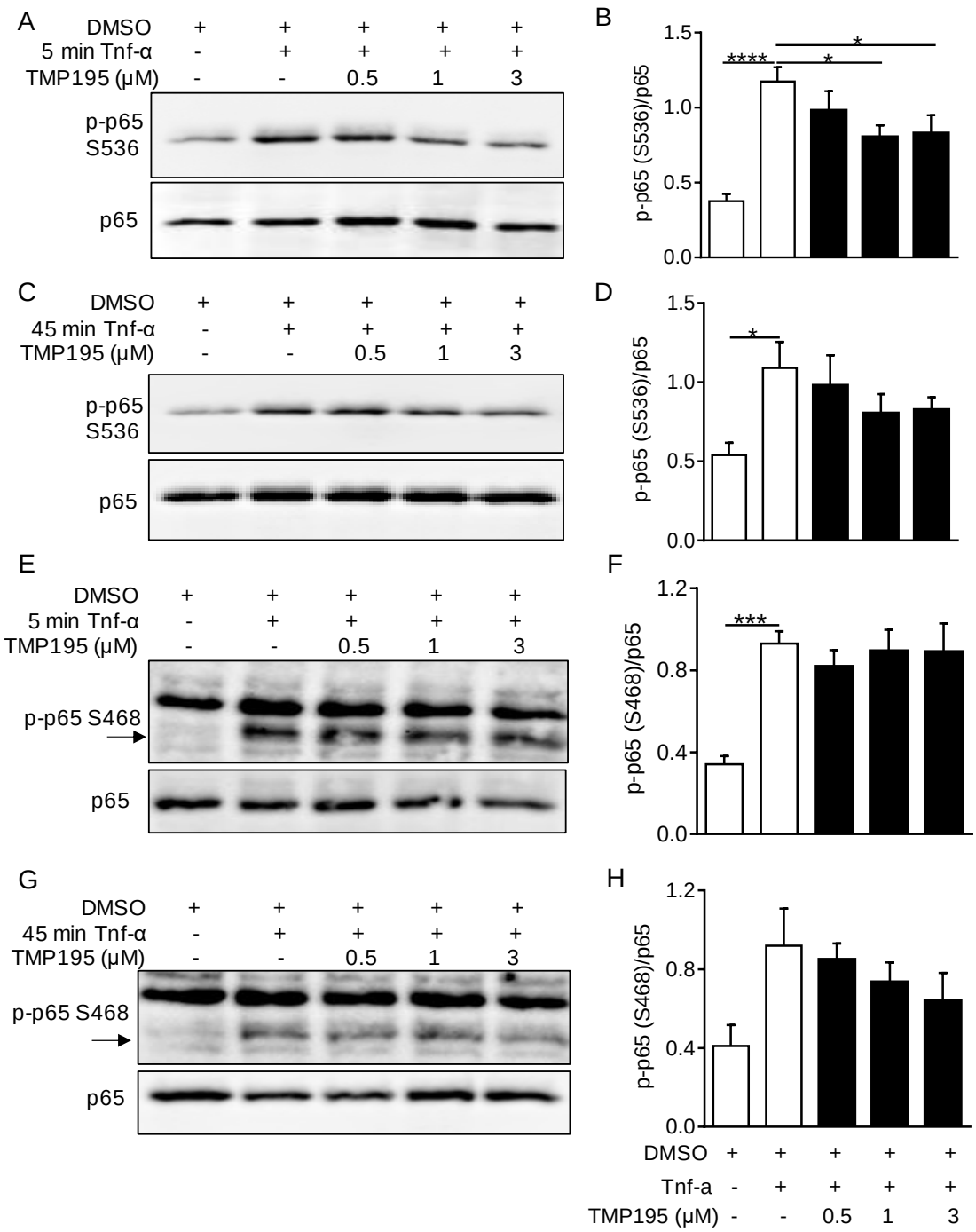

Figure 17. TMP195 treatment of Tnf-α stimulated BMDMs reduces p65 phosphorylation at serine residue 536.

BMDMs were generated from *Apoe*$^{-/-}$ mice and treated with TMP195 in different concentrations or DMSO (vehicle) and either stimulated with Tnf-α (50 ng/mL) for 5 (A, B, E, F) or 45 min (C, D, G, H) or left untreated. (A) and (C) show representative immunoblots and (B) and (D) show quantifications of phosphorylated p65 at serine 536 and normalized to total p65 with n = 8 independent experiments. (E) and (G) show representative immunoblots and (F) and (H) show quantifications of phosphorylated p65 at serine 468 and normalized to total p65 with n = 4-5 independent experiments. Data represent means ± SEM. One-way ANOVA with Holm-Sidak

post-test for comparison of TMP195 vs. Vehicle control*:* *, p<0.05; **, p<0.01; ***, p<0.001; ****, p<0.0001.

4.5.3 TMP195 attenuates atherosclerotic lesion development in Apoe$^{-/-}$ mice in vivo

The next step was to examine effects of TMP195 on atherosclerotic lesion development *in vivo.* 6-7 weeks old male *Apoe*$^{-/-}$ mice received daily i.p. injections of TMP195 (50 mg/kg) or DMSO (Vehicle) for 4 weeks and in parallel were fed a high fat western-diet to accelerate atherosclerosis (Figure 18 A). Hearts were cut and stained with Oil-Red O and Hematoxylin for analysis of plaques in the aortic valve of n = 11-12 mice per group. Quantification of absolute lesion area and relative lesion size in comparison to total aortic root showed reduced early lesion development in mice treated with TMP195 (Figure 18 B- D).

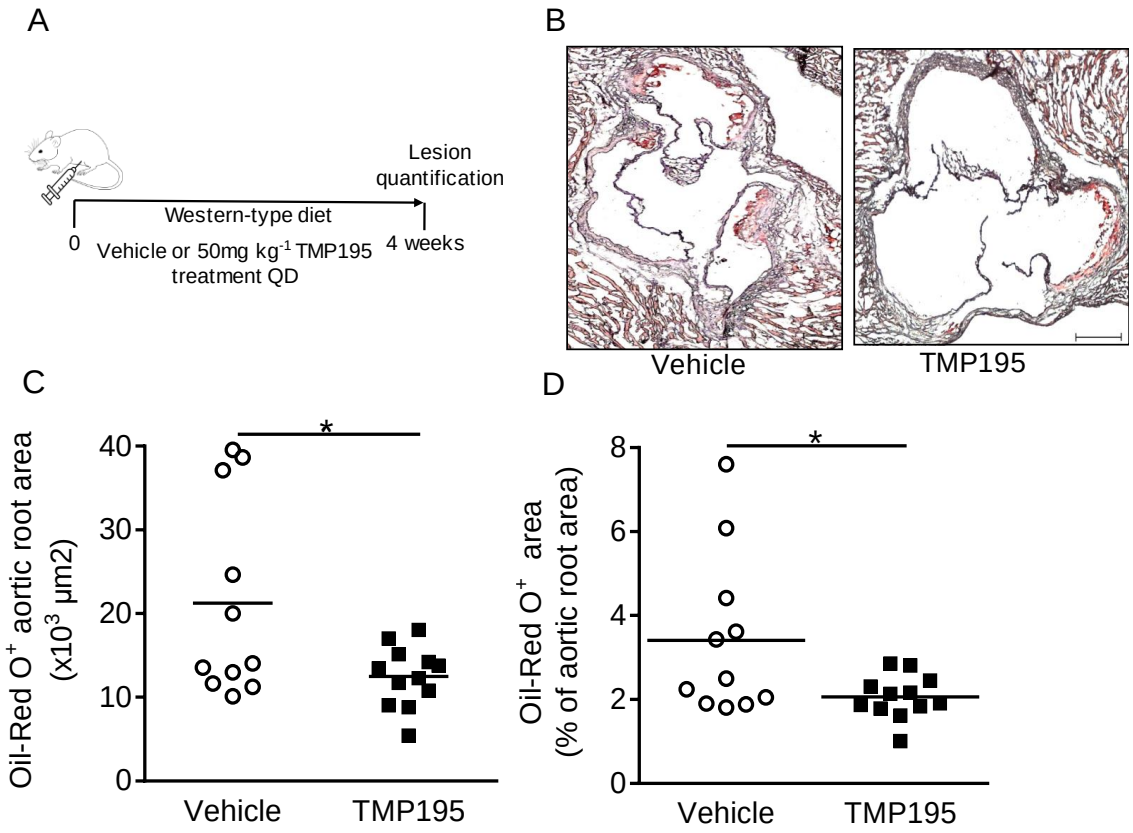

Figure 18. TMP195 treatment attenuates atherosclerotic lesions in *Apoe*$^{-/-}$ mice *in vivo.*

Experimental design for *in vivo* TMP195 treatment of *Apoe*$^{-/-}$ mice (A): 6-7 weeks old male Apoe$^{-/-}$ mice were given daily i.p. injections of DMSO (Vehicle) or TMP195 (50mg/kg) for 4 weeks while receiving a Western-type diet in parallel. Aortic roots of TMP195 or Vehicle treated *Apoe*$^{-/-}$ mice for n = 11-12 mice in a group were then stained with Oil Red-O and atherosclerotic lesion development was quantified for absolute lesion size (C) and relative lesion area (D). Representative images are shown in (B) with scale bars representing 200µm. Data represent

means ± SEM. Unpaired t-test with Welch's correction or Mann-Whitney test, as appropriate, for comparison of TMP195 vs. Vehicle control: *, $p<0.05$.

Taken together, these results indicate an atheroprotective and anti-inflammatory effect of TMP195 treatment in Tnf-α stimulated *Apoe*-deficient macrophages and mice.

4.6 Selective pharmacological class IIa HDAC inhibition has anti-inflammatory effects in human monocytes

The observation that TMP195 treatment has an anti-inflammatory and atheroprotective effect in *Apoe*-deficient mice and isolated murine macrophage cells prompted us to further examine the effects of the inhibitor in human monocytes.

4.6.1 Ex vivo TMP195 treatment limits pro-inflammatory responses in TNF-α stimulated human monocytes from healthy donors

First, we investigated the effects of *ex vivo* TMP195 treatment in healthy human monocytes. After collecting blood from healthy volunteers from the laboratory, monocytes were isolated and then incubated with different concentrations of TMP195 (0.5, 1, 3 or 5 µM) or DMSO (Vehicle) and stimulated with human TNF-α for 24 h or left untreated. We demonstrated that TMP195 inhibited cytokine production of IL-8, IL-6 as well as IL1-β and CCL2 leaving TNF-α levels unaffected (Figure 19 A- E).

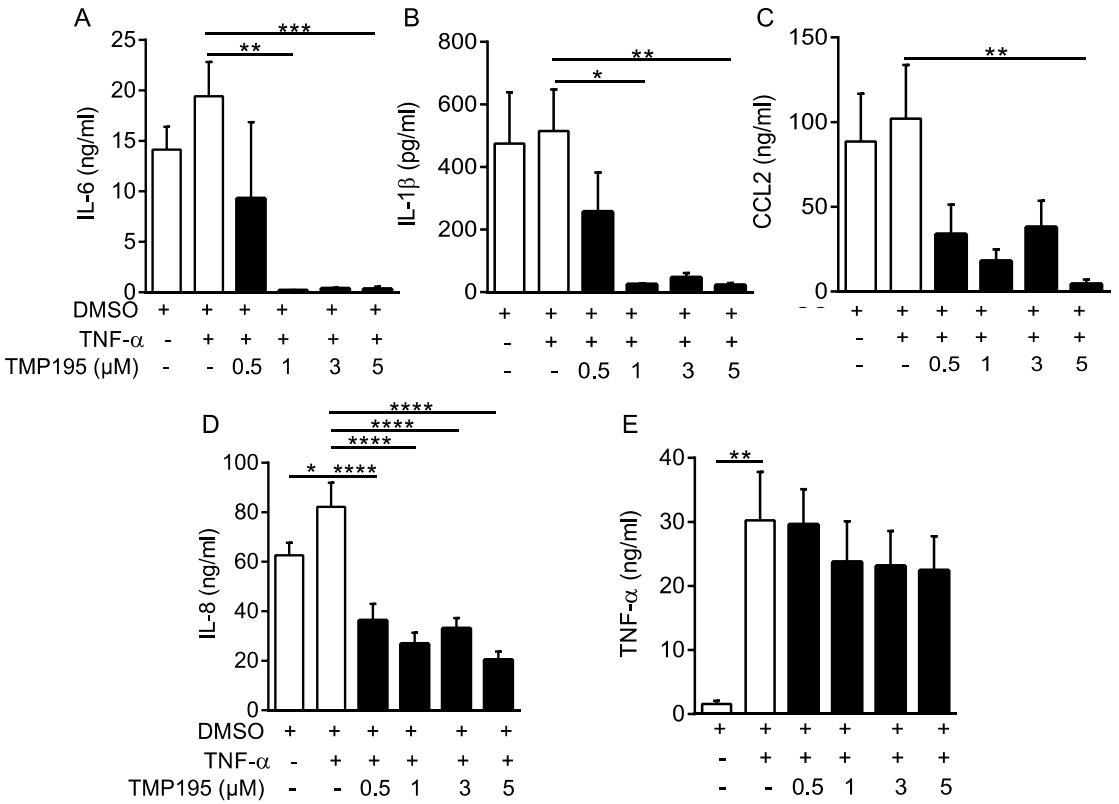

Figure 19. *Ex vivo* TMP195 treatment limits pro-inflammatory responses in TNF-α stimulated monocytes from healthy donors.

Monocytes were isolated from healthy donors by Ficoll-Paque and magnetic labeling and pretreated with increasing concentrations of TMP195 (0.5, 1, 3 or 5 μM) or DMSO (vehicle) for 1h and were either stimulated with TNF-α for 24h or left untreated. Supernatants were collected and used for protein analysis of IL-6 (A), IL-1β (B), CCL2 (C), IL-8 (D) and TNF-α (E) with ELISA for n = 5-6 healthy donors (ages 23 – 51 years old). Data represent means ± SEM. One-way ANOVA with Holm-Sidak multiple comparison test or Kruskal-Wallis with Dunn's multiple comparison test, as appropriate, for comparison of TMP195 vs. Vehicle control: *, p<0.05; **, p<0.01; ***, p<0.001; ****, p<0.0001.

4.6.2 TMP195 treatment limits pro-inflammatory responses in TNF-α-stimulated human monocytes from patients with atherosclerosis manifestation

Next, with anti-inflammatory effects of TMP195 treatment in healthy human monocytes, it was of great interest to likewise study the effects of TMP195 in monocytes from patients with atherosclerosis manifestation. Selection of patients was based on ultrasound confirmed presence of carotid artery stenosis or atherosclerotic plaques in the carotid artery (Table 9 shows demographic details and extracranial carotid duplex ultrasound findings). The experimental setup was the same as described before. ELISA analysis of the collected supernatant

showed significantly reduced protein levels in 5 µM pretreated monocytes for IL-6, IL-1β and CCL2 (Figure 20 A-C), although IL-8 and TNF-α did not show any significant differences (Figure 20 D, E).

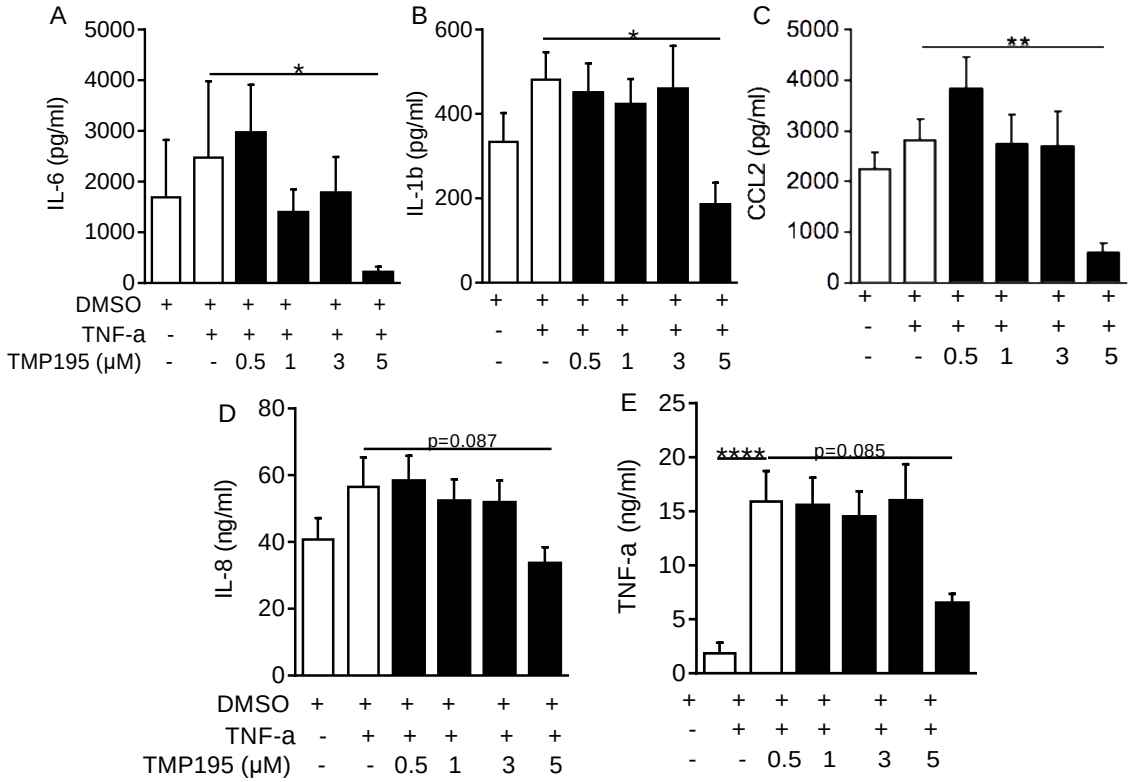

Figure 20. *Ex vivo* TMP195 treatment limits pro-inflammatory responses in TNF-α stimulated monocytes from patients with carotid atherosclerosis.

Monocytes were isolated from patients with carotid artery plaques or stenosis by Ficoll-Paque and magnetic labeling and pretreated with increasing concentrations of TMP195 (0.5, 1, 3 or 5 µM) or DMSO (vehicle) for 1 h and were either stimulated with TNF-α for 24 h or left untreated. Supernatants were collected and used for protein analysis of IL-6 (A), IL1-β (B), CCL2 (C), IL-8 (D) and TNF-α (E) with ELISA for n = 12 patients. Data represent means ± SEM. One-way ANOVA with Holm-Sidak multiple comparison test or Kruskal-Wallis with Dunn's multiple comparison test, as appropriate, for comparison of TMP195 vs. Vehicle control*:* *, p<0.05; **, p<0.01; ***, p<0.001; ****, p<0.0001.

Together, these results suggest an anti-inflammatory effect of TMP195 in human monocytes - from healthy donors as well as from donors with carotid atherosclerosis.

5 Discussion

Genome-wide association studies identified the HDAC9 gene region as a major genetic risk factor for large-vessel stroke (LVS), but also for other cardiovascular diseases (CVD) such as aortic atherosclerotic calcification, coronary artery disease (CAD) and peripheral artery disease (PAD). The underlying pathology of all these highly prevalent diseases is atherosclerosis, a chronic inflammatory disease of the vessel walls. Hence, HDAC9 is an attractive therapeutic target in prevention of vascular inflammation and its clinical manifestation of stroke and other CVDs. Yet, the mechanisms linking HDAC9 to vascular inflammation and the ensuing therapeutic potential are insufficiently defined.

In this thesis we show that: **(1)** HDAC9 enhances pro-inflammatory responses *in vivo* as well as *in vitro* in primary macrophages, which have a defined pivotal role in atherogenesis; **(2)** *Hdac9* deficiency limits NF-κB activity in macrophages and monocytes, suggesting that Hdac9 promotes the activation of NF-κB signaling thus, identifying the NF-κB pathway as a downstream effector of Hdac9; and **(3)** treatment with the class IIa specific HDAC inhibitor TMP195 attenuates atherosclerotic lesion formation and leads to limited pro-inflammatory responses in human monocytes from both healthy donors and patients with carotid atherosclerosis. Therefore, therapeutic HDAC9 inhibition is a promising novel strategy for atheroprotection and prevention of vascular inflammation in humans with great clinical importance.

5.1 HDAC9 enhances pro-inflammatory responses

The conclusion that HDAC9 enhances pro-inflammatory responses is based on several observations demonstrated in this thesis. *Hdac9* deficiency resulted in a reduction of leukocyte recruitment and pro-inflammatory cytokines in the murine peritoneum under acute and chronic inflammatory conditions *in vivo* and a reduction of pro-inflammatory molecules in BMDMs *in vitro* and peritoneal macrophages *in vivo*.

To simulate acute inflammatory conditions experimentally, we stimulated with either LPS, the most abundant component within gram-negative bacterial cell wall [110], or with Tnf-α, an endogenous pyrogen with a variety of biological effects

on many cells. Systemically, TNF-α leads to fever and acute phase reaction of the body while locally it induces the production of endogenous inflammation mediators, leukocyte activation and apoptosis [111, 112]. Thus, when injecting the murine peritoneum with LPS or Tnf-α, it strongly mimics a state of acute inflammation in the tissue. In our study, peritoneal exudate obtained from LPS-stimulated *Hdac9*$^{-/-}$*Apoe*$^{-/-}$ mice showed, compared to the peritoneum of their *Hdac9*$^{+/+}$*Apoe*$^{-/-}$ control littermates, a significantly reduced number of leukocytes and also reduced amounts of pro-inflammatory molecules, especially for levels of Tnf-α and Cxcl1. Hence, this suggests reduced chemokine- and cytokine-dependent cell migration to the site of inflammation. Typically, when exposed to inflammation or injury, multifarious leukocytes like neutrophil granulocytes, lymphocytes and monocytes are rapidly recruited to the site of inflammation through chemokine and cytokine stimulated chemotaxis, and accumulate there. Normally, as critical part of the host's innate immune mechanism, responses in acute inflammation are self-limiting through phagocytic resolution of inflammatory cells [113]. In the case of atherosclerosis, there is dysregulation of this process and hence failure of acute inflammation resolution resulting in chronic inflammation with persistent inflammatory stimuli and processes [114]. The phenotype demonstrated here indicates a pro-inflammatory role of Hdac9 in early acute stages of inflammation. Our results are in accordance with similar conclusions from previous studies in Hdac9-depleted LDLr$^{-/-}$mice that showed reduced secretion of pro-inflammatory cytokines in macrophages after LPS stimulation as well as upregulated cholesterol efflux genes such as ABCA1 and ABCG1 [67]. Furthermore, *Hdac9* deficiency was shown to result in phenotype shifting in macrophages with more anti-inflammatory M2 and less pro-inflammatory M1 macrophages [67], which again highlights the pro-inflammatory role of HDAC9. A possible explaination as to why some cytokines like Cxcl1, Il1-β and Ccl2 remained unaffected in our study may lie in the multifarious composition of resident and influxed cells in the peritoneum with diverse activation of downstream promotor elements upon stimulation.

When feeding *Apoe*$^{-/-}$ mice a chow diet for 28 weeks, it mimics the state of a chronic inflammation with the presence of advanced atherosclerotic lesions (Figure 3, Chapter 1.2.3). The analysis in this thesis showed that in this chronic

state of inflammation, there is significant reduction of circulating pro-inflammatory Cxcl1 levels in *Hdac9*-deficient mice. This further corroborates the anti-inflammatory effects elicited by *Hdac9* deficiency. Collectively, these results obtained in both inflammatory models suggest a promoting role of HDAC9 on multiple levels of the inflammatory cascade in both acute as well as more advanced stages of atheroprogression.

Multifarious cell-types are involved in the pathophysiology of atherosclerosis such as smooth muscle cells, endothelial cells, monocytes and macrophages [25]. Function of individual HDACs in atherosclerosis is multifactorial with differential roles in multiple atherosclerosis-relevant cell types [55, 57]. For example, HDAC1 has repressive effects on NF-κB signaling in macrophages [97, 115], while HDAC3 has activating effects on NF-κB signaling in the same cell type [116]. As discussed above, monocytes and macrophages are key drivers in the pathogenesis of atherosclerosis and the main focus of this thesis. As demonstrated in *in vivo* peritoneal macrophages as well as *in vitro* BMDMs, the results of this thesis clearly suggest a pro-inflammatory role of HDAC9 in these cells pivotal for atherosclerosis. We showed limited pro-inflammatory responses in *Hdac9*-deficient and either LPS or Tnf-α stimulated BMDMs for Cxcl1, Ccl2, Il1-β and Tnf-α. These are all pro-inflammatory cytokines and chemokines known to have defined functions in different stages of atherosclerosis. While Cxcl1 and Ccl2 are chemokines mostly involved in rolling, capture and transmigration of monocytes [23], hence important for initiation of atherosclerotic plaques, Il1-β is important in plaque progression and rupture [117]. For Tnf-α, one of the most potent endogenous pro-inflammatory cytokines, numerous studies showed that its deficiency resulted in decreased foam cells, reduced expression of several pro-inflammatory cytokines and diminished formation of fatty streak lesions in ApoE-deficient mice [118-120]. Only Il-6 remained unaffected in our results which may be due to its ambivalent, both pro- and anti-inflammatory effects described in literature. On one hand, Il-6 has been shown to exacerbate atherosclerosis by increasing pro-inflammatory cytokines and lesion size and decreasing plaque stability [121, 122]. Correspondingly, *Il-6* deficiency was shown to have atheroprotective effects in both *Apoe*$^{-/-}$ and *LDLr*$^{-/-}$ mice [123]. In contrast, other studies reported that *Il-6*–deficient mice developed more atherosclerotic lesions

in advanced stages [122]. Thus, Il-6 has both atheroprotective and atheropromoting effects.

The *in vivo* relevance of our results is demonstrated by accordant results in peritoneal macrophages retrieved from LPS-injected mice. Here, reduced gene expression for mRNA levels of analyzed pro-inflammatory cytokines was shown in *Hdac9*-deficient mice. Comparing the results obtained from the peritoneal exudate versus from peritoneal macrophages, we observed discrepancy in the pattern of affected pro-inflammatory cytokines. This observed difference might be explained by the presence of a variety of inflammation-triggered cells in the inflammatory peritoneum. Hence, the stimulated peritoneal exudate consists of secreted cytokines not only from macrophages, but combined secretion from different resident and influxed cells in the peritoneum with diverse activation of downstream promotor elements upon stimulation. For further understanding, concordant experiments in other cell types extremely relevant to inflammation and atherosclerosis, like vascular smooth muscle cells or endothelial cells, are highly of interest and currently part of another ongoing research in our group.

5.2 Hdac9 has activating effects on NF-κB phosphorylation and activity – Identifying NF-κB as downstream effector of HDAC9

We found protein levels of several pro-inflammatory genes linked to NF-κB, like Tnf-α or Il1-β, to be elevated by Hdac9. Hence, it is highly promising to investigate the involvement of Hdac9 in the NF-κB pathway.

The results demonstrated in this thesis reveal an activating effect of Hdac9 on NF-κB signaling in BMDMs, thus identifying the NF-κB signaling pathway as a downstream effector of Hdac9 underlying its pro-inflammatory and pro-atherogenic effects. This is supported by the observation that under inflammatory conditions, *Hdac9* deficiency resulted in

(a) an inhibition of phosphorylation at serine residues 536 and 468 and

(b) a decrease in *de novo* synthesis of IκB-α.

In previous studies, cross-talk between HDACs and NF-κB signaling are mostly described in epithelial cells and immortalized T lymphocytes and predominantly involve class I HDACs (HDAC 1, 2 and 3), which were primarily shown to directly

associate with p65 in the nucleus and to mostly repress NF-κB signaling [95-97]. Our findings significantly add to these observations by showing that HDAC9 promotes NF-κB activity in macrophages. HDAC9 is already known to act as a kinase activator with direct enzymatic activity through deacetylation of TBK1. Other class IIa HDACs, however, are mostly known to primarily control gene expression through recruitment of other corepressors or coactivators [55] with only limited catalytic activity. Hence, it is of high interest to explore whether HDAC9 directly interacts with NF-κB pathway molecules such as kinases upstream of the observed HDAC9-dependent downregulation of NF-κB phosphorylation and activity. Ultimately, the aim is to identify the link between HDAC9 and NF-κB pro-inflammatory atherogenic processes.

NF-κB activity is regulated by phosphorylation of its subunits, particularly p65. Dependent on the kinases and specific residues involved, phosphorylation of p65 either enhances or diminishes NF-κB activity. Phosphorylation of p65 at serine residue 536 or serine residue 468, both located in the transactivation domain, leads to enhancement of NF-κB transactivation in a target gene-specific manner (‘barcode’ hypothesis) [84]. We showed that in BMDMs from *Hdac9*-deficient mice, p65 phosphorylation of both serine residues was reduced after certain durations of inflammatory stimulation. For LPS, the results suggest effects at prolonged time points of stimulation. In conclusion, HDAC9 is required for sustained phosphorylation of p65 at both serine residues 536 and 468. Since p65 phosphorylation activates NF-κB-dependent gene translation of a wide variety of pro-atherogenic genes, this is consistent with our demonstrated results of HDAC9-dependent pro-inflammatory effects on inflammatory cytokines and chemokines. Some of these target genes, however, are also controlled by other promoter elements such as Ccl2 expression being co-driven by activator protein-1 (AP-1) [124]. This could explain why some well-described targets of NF-κB remained unaffected in our results, as also described in another study before [125].

Known kinases to phosphorylate serine 536 include non-canonical kinases like TBK1, IKKε, IKKα or IKKβ [63, 98]. IKKε and IKKβ are both also associated with serine 468 phosphorylation. As described above, HDAC9 has direct physical interaction with TBK1 [63]. Given the established activating effect of HDAC9 on

NF-κB signaling [126], TBK1 could represent a possible link between HDAC9 and atherosclerosis through modulation of p65 phosphorylation and the NF-κB signaling pathway. However, TBK1 has not been associated with phosphorylation of serine 468 which suggests the possible involvement of additional kinases that remain to be identified and further explored. It would also be of interest to further investigate a possible link between HDAC9 and IKKβ, especially as it is associated with both serine 536 and serine 468 and plays an important role in mediating p65 phosphorylation [98].

A critical step in NF-κB signaling pathway is the negative feedback loop through NF-κB-dependent *de novo* synthesis of IκB-α. Post stimulation, IκB-α accumulates intranuclearly to induce nuclear export of NF-κB, hence terminating binding to the DNA and NF-κB-activated gene transcription. We demonstrated reduced cytoplasmic *de novo* IκB-α levels after stimulation, which can be explained with the overall reduction of NF-κB activation through *Hdac9* deficiency. Previous studies also described a HDAC inhibitor-dependent delayed cytoplasmic reappearance of IκB-α after TNF-stimulation [127]. However, Adam *et al.* [127] suggested that the delay resulted from a persistent degradation of the IκB-α protein. In contrast, in our experiments *Hdac9* deficiency did not show any effects on IκB-α degradation as levels of phosphorylated IκB-α were unaffected. It is known that IκB-α phosphorylation is the first step needed for polyubiquination and ubiquitin-mediated proteolysis of IκB-α [91]. A possible explanation for this discrepancy is that Adam *et al.* used TSA, a broad HDAC inhibitor, while our experiments are results of specific *Hdac9* knockout experiments. On another note, in our experiments basal IκB-α level remained unchanged in *Hdac9*-deficient mice which suggests that HDAC9 does not regulate basal IκB-α activity in primary macrophages.

5.3 Selective pharmacological inhibition of class IIa HDACs has atheroprotective and anti-inflammatory effects in mice and *ex vivo* human monocytes

TMP195 is a selective class IIa HDAC inhibitor [80]. Further data provided by Guerriero *et al*. [81] showed that TMP195 promotes an anti-tumor innate immune

response by predominantly affecting monocytes and macrophages while other cell types like lymphocytes showed minimal response. In our experiments using TMP195, we could show that

(a) TMP195 treatment in BMDMs under inflammatory conditions resulted in reduced pro-inflammatory cytokine production and abridged sustained p65 phosphorylation. Importantly, we demonstrated that

(b) pretreatment with TMP195 attenuates atherogenic lesion development in western-type diet fed *Apoe*$^{-/-}$ mice and limits the pro-inflammatory milieu in PBMCs isolated from both healthy donors and patients with atherosclerosis.

These results with TMP195 are consistent with our previous data obtained in the *Hdac9* knockout mice, highlighting a pro-inflammatory role of HDAC9. Hence, this inhibitor provides a promising therapeutic perspective for prevention of vascular inflammation and its clinical manifestations.

For many years now, HDAC inhibitors have been studied for therapeutic use in multifarious fields such as inflammation, cancer and autoimmunity [56, 78]. Few HDAC inhibitors, such as vorinostat (SAHA) and romidepsin (FK288), have been approved for clinical use, but exclusively for treatment of hematological cancers like cutaneous T-cell lymphoma or multiple myeloma [128]. However, these currently clinically applied HDAC inhibitors lack selectivity among HDAC isoforms. Given the specific and even antagonistic effects of individual HDACs in atherosclerosis, it is unsurprising that use of broad-spectrum HDAC inhibitors have shown evidence of contraindications in its use for cardiovascular disease [79]. For example, use of TSA, which broadly inhibits the HDAC isoforms 1, 3, 4, 6 and 10, leads to exacerbation of atherosclerosis lesion size in *LDLr*-deficient mice [79], despite its clearly documented anti-atherogenic effect in macrophages [129]. In conclusion, these observations highlight the importance of specific pharmaceutical HDAC inhibition. [9, 130, 131]. Nonetheless, our results using TMP195 are consistent with studies exploring broad spectrum HDAC inhibitors like TSA, givinostat (ITF2357) and SAHA, which also describe inhibiting effects on inflammatory cytokine production in different cell types including BMDMs and PBMCs [132-134]. In addition, some of these HDAC inhibitors also have downregulating effects on NF-κB activation in PBMCs [135]. In contrast, in epithelial cells use of HDAC inhibitors leads to potentiation instead of attenuation

of NF-κB activation [127]. This might relate to a cell type-specific regulation of NF-κB activity by HDACs. Furthermore, our experiment showed that TMP195 downregulated p65 phosphorylation at serine 536, but not 468. This suggests a phosphorylation site-specific regulation of NF-κB activity by different HDACs.

As demonstrated in Chapter 4.5.2, we showed attenuation of early lesion development in the aortic valve of *Apoe*-deficient mice attributed to the use of TMP195. This highlights the importance of TMP195 in its role to confer atheroprotection, especially in the early stages of atherosclerosis initiation. However, secondary prophylactic treatment in cardiovascular risk patients is mostly initiated at a state where atherosclerotic lesions already exist. Hence, it would be of high interest to assess whether there are also therapeutic effects of TMP195 on atheroprogression when there is already manifested atherosclerosis. Our *ex vivo* data in human monocytes showed that TMP195 also reduced the levels of pro-inflammatory cytokines from patients with atherosclerosis. This underlines the importance of HDAC9 as a promising target for further therapeutic and interventional studies in humans, especially in the population with increased cardiovascular risk. Interestingly, effects of TMP195 appear to be without clear dose responsiveness in a ‘all or nothing’ manner. However, mechanism mediating this effect remain yet to be explored.

All taken together, the need to target multiple atherosclerosis-relevant cell types while only inhibiting specific HDACs becomes strongly apparent. Our findings with use of TMP195 overcomes the limitations from the use of broad-spectrum HDAC inhibitors. Nonetheless, it is important to develop class IIa HDAC inhibitors with even higher specificity for HDAC9. Furthermore, cytotoxicity and side effects need to be further explored as studies using SAHA and romidepsin revealed significant limitations due to substantial toxicity in T-cell lymphoma patients such as cardiotoxicity and hypercholesterolemia [136]. Although TMP195 did not show relevant cell toxicity in mice [81], side effects may still occur and remain to be explored.

In conclusion, several observations from this study as well as from previous studies define inhibition of HDAC9 as a promising strategy to prevent atherosclerosis:

(a) the discovery of the *HDAC9* gene region as a major risk locus for atherosclerotic phenotypes in humans [13, 14, 16, 17];

(b) the beneficial effect of *Hdac9* deficiency on inflammation in mice [9, 67]; and

(c) all the results obtained here in different *in vivo and in vitro* HDAC9-targeting including *Hdac9* knockout and *in vivo* use of TMP195 in mice and *ex vivo* TMP195 treatment of human monocytes.

6 List of Abbreviations

Ab	antibody
Apoe	apolipoprotein e
BSA	bovine serum albumin
BMDMs	bone marrow derived macrophages
CAD	coronary artery disease
CVD	cardiovascular disease
Cxcl1	chemokine (C-X-C-motif) ligand 1
Ccl2	CC-Chemokin-Ligand-2
cDNA	complementary DNA
DMSO	dimethyl sulfoxide
DTT	dithiothreitol
ELISA	enzyme-linked immunosorbent assay
ECs	endothelial cells
FCS	fetal calf serum
GAPDH	glyceraldehyde 3-phosphate dehydrogenase
GWAS	genome-wide association study
HDAC	histone deacetylase
HDACi	histone deacetylase inhibitor
ICAM-1	intercellular adhesion molecule 1
IKK	inhibitor of kappa B Kinase
IκB-α	NF-kappa-B inhibitor alpha-like
IL1-β	Interleukin-1β
IL-6	Interleukin-6
IL-10	Interleukin-10
i.p.	intraperitoneally
kDa	kilodalton
KO	knockout
LCM	L929-cell-conditioned medium
LDL	low density lipoprotein
LPS	lipopolysaccharide
LVS	large-vessel stroke
MCSF	mouse colony stimulating factor

MIF	macrophage migration inhibitory factor
mTNFα	murine tumor necrosis factor
NF-κB	nuclear factor kappa-light-chain enhancer of activated B cell
oxLDL	oxidized low density lipoprotein
PBS	phosphate buffered saline
PBMCs	peripheral blood mononuclear cells
PTMs	posttranslational modifications
PAD	peripheral artery disease
q-PCR	quantitative real time polymerase chain reaction
RNA	ribonuclease acid
SMCs	smooth muscle cells
SNP	single-nucleotide polymorphism
TAD	transactivation domain
TBK1	TANK-binding kinase-1
TNF	tumor necrosis factor
WT	wild-type
WTD	western-type diet

7 List of Figures and Tables

7.1 List of Figures

7.2 List of Tables

8 References

1. Sacco, R.L., et al., *An updated definition of stroke for the 21st century: a statement for healthcare professionals from the American Heart Association/American Stroke Association.* Stroke, 2013. **44**(7): p. 2064-89.

2. Collaborators, G.B.D.C.o.D., *Global, regional, and national age-sex specific mortality for 264 causes of death, 1980-2016: a systematic analysis for the Global Burden of Disease Study 2016.* Lancet, 2017. **390**(10100): p. 1151-1210.

3. Collaborators, G.B.D.L.R.o.S., et al., *Global, Regional, and Country-Specific Lifetime Risks of Stroke, 1990 and 2016.* N Engl J Med, 2018. **379**(25): p. 2429-2437.

4. DALYs, G.B.D. and H. Collaborators, *Global, regional, and national disability-adjusted life-years (DALYs) for 333 diseases and injuries and healthy life expectancy (HALE) for 195 countries and territories, 1990-2016: a systematic analysis for the Global Burden of Disease Study 2016.* Lancet, 2017. **390**(10100): p. 1260-1344.

5. Heuschmann, P., et al., *Schlaganfallhäufigkeit und Versorgung von Schlaganfallpatienten in Deutschland.* Aktuelle Neurologie, 2010. **37**(07): p. 333-340.

6. Amarenco, P., et al., *Classification of stroke subtypes.* Cerebrovasc Dis, 2009. **27**(5): p. 493-501.

7. Adams, H.P., Jr., et al., *Classification of subtype of acute ischemic stroke. Definitions for use in a multicenter clinical trial. TOAST. Trial of Org 10172 in Acute Stroke Treatment.* Stroke, 1993. **24**(1): p. 35-41.

8. Kolominsky-Rabas, P.L., et al., *Time trends in incidence of pathological and etiological stroke subtypes during 16 years: the Erlangen Stroke Project.* Neuroepidemiology, 2015. **44**(1): p. 24-9.

9. Azghandi, S., et al., *Deficiency of the stroke relevant HDAC9 gene attenuates atherosclerosis in accord with allele-specific effects at 7p21.1.* Stroke, 2015. **46**(1): p. 197-202.

10. Dichgans, M., *Genetics of ischaemic stroke.* Lancet Neurol, 2007. **6**(2): p. 149-61.

11. Dichgans, M., et al., *Shared genetic susceptibility to ischemic stroke and coronary artery disease: a genome-wide analysis of common variants.* Stroke, 2014. **45**(1): p. 24-36.

12. Bevan, S., et al., *Genetic heritability of ischemic stroke and the contribution of previously reported candidate gene and genomewide associations.* Stroke, 2012. **43**(12): p. 3161-7.

13. International Stroke Genetics, C., et al., *Genome-wide association study identifies a variant in HDAC9 associated with large vessel ischemic stroke.* Nat Genet, 2012. **44**(3): p. 328-33.

14. Traylor, M., et al., *Genetic risk factors for ischaemic stroke and its subtypes (the METASTROKE collaboration): a meta-analysis of genome-wide association studies.* Lancet Neurol, 2012. **11**(11): p. 951-62.

15. Malik, R., et al., *Multiancestry genome-wide association study of 520,000 subjects identifies 32 loci associated with stroke and stroke subtypes.* Nat Genet, 2018. **50**(4): p. 524-537.

16. Consortium, C.A.D., et al., *Large-scale association analysis identifies new risk loci for coronary artery disease.* Nat Genet, 2013. **45**(1): p. 25-33.

17. Matsukura, M., et al., *Genome-Wide Association Study of Peripheral Arterial Disease in a Japanese Population.* PLoS One, 2015. **10**(10): p. e0139262.

18. Malhotra, R., et al., *HDAC9 is implicated in atherosclerotic aortic calcification and affects vascular smooth muscle cell phenotype.* Nat Genet, 2019. **51**(11): p. 1580-1587.

19. Moore, K.J. and I. Tabas, *Macrophages in the pathogenesis of atherosclerosis.* Cell, 2011. **145**(3): p. 341-55.

20. Weber, C. and H. Noels, *Atherosclerosis: current pathogenesis and therapeutic options.* Nat Med, 2011. **17**(11): p. 1410-22.

21. Ramji, D.P. and T.S. Davies, *Cytokines in atherosclerosis: Key players in all stages of disease and promising therapeutic targets.* Cytokine Growth Factor Rev, 2015. **26**(6): p. 673-85.

22. Dornquast, C., et al., *Regional Differences in the Prevalence of Cardiovascular Disease.* Dtsch Arztebl Int, 2016. **113**(42): p. 704-711.

23. Moore, K.J., F.J. Sheedy, and E.A. Fisher, *Macrophages in atherosclerosis: a dynamic balance.* Nat Rev Immunol, 2013. **13**(10): p. 709-21.

24. Gimbrone, M.A., Jr. and G. Garcia-Cardena, *Vascular endothelium, hemodynamics, and the pathobiology of atherosclerosis.* Cardiovasc Pathol, 2013. **22**(1): p. 9-15.

25. Hansson, G.K. and P. Libby, *The immune response in atherosclerosis: a double-edged sword.* Nat Rev Immunol, 2006. **6**(7): p. 508-19.

26. Weber, C., A. Zernecke, and P. Libby, *The multifaceted contributions of leukocyte subsets to atherosclerosis: lessons from mouse models.* Nat Rev Immunol, 2008. **8**(10): p. 802-15.

27. Lusis, A.J., *Atherosclerosis.* Nature, 2000. **407**(6801): p. 233-41.

28. Zheng, X.X., et al., *Histone deacetylases and atherosclerosis.* Atherosclerosis, 2015. **240**(2): p. 355-66.

29. Smith, J.D., et al., *Decreased atherosclerosis in mice deficient in both macrophage colony-stimulating factor (op) and apolipoprotein E.* Proc Natl Acad Sci U S A, 1995. **92**(18): p. 8264-8.

30. Libby, P., *Inflammation in atherosclerosis.* Arterioscler Thromb Vasc Biol, 2012. **32**(9): p. 2045-51.

31. Steinl, D.C. and B.A. Kaufmann, *Ultrasound imaging for risk assessment in atherosclerosis.* Int J Mol Sci, 2015. **16**(5): p. 9749-69.

32. Tabas, I. and K.E. Bornfeldt, *Macrophage Phenotype and Function in Different Stages of Atherosclerosis.* Circ Res, 2016. **118**(4): p. 653-67.

33. Ley, K., et al., *Getting to the site of inflammation: the leukocyte adhesion cascade updated.* Nat Rev Immunol, 2007. **7**(9): p. 678-89.

34. Soehnlein, O., et al., *Distinct functions of chemokine receptor axes in the atherogenic mobilization and recruitment of classical monocytes.* EMBO Mol Med, 2013. **5**(3): p. 471-81.

35. Ley, K., Y.I. Miller, and C.C. Hedrick, *Monocyte and macrophage dynamics during atherogenesis.* Arterioscler Thromb Vasc Biol, 2011. **31**(7): p. 1506-16.

36. Geissmann, F., S. Jung, and D.R. Littman, *Blood monocytes consist of two principal subsets with distinct migratory properties.* Immunity, 2003. **19**(1): p. 71-82.

37. Tacke, F., et al., *Monocyte subsets differentially employ CCR2, CCR5, and CX3CR1 to accumulate within atherosclerotic plaques.* J Clin Invest, 2007. **117**(1): p. 185-94.

38. Woollard, K.J. and F. Geissmann, *Monocytes in atherosclerosis: subsets and functions.* Nat Rev Cardiol, 2010. **7**(2): p. 77-86.

39. Sica, A. and A. Mantovani, *Macrophage plasticity and polarization: in vivo veritas.* J Clin Invest, 2012. **122**(3): p. 787-95.

40. Leitinger, N. and I.G. Schulman, *Phenotypic polarization of macrophages in atherosclerosis.* Arterioscler Thromb Vasc Biol, 2013. **33**(6): p. 1120-6.

41. Wolfs, I.M., M.M. Donners, and M.P. de Winther, *Differentiation factors and cytokines in the atherosclerotic plaque micro-environment as a trigger for macrophage polarisation.* Thromb Haemost, 2011. **106**(5): p. 763-71.

42. Rahman, K., et al., *Inflammatory Ly6Chi monocytes and their conversion to M2 macrophages drive atherosclerosis regression.* J Clin Invest, 2017. **127**(8): p. 2904-2915.

43. Leibovich, S.J. and R. Ross, *The role of the macrophage in wound repair. A study with hydrocortisone and antimacrophage serum.* Am J Pathol, 1975. **78**(1): p. 71-100.

44. Rutherford, M.S., A. Witsell, and L.B. Schook, *Mechanisms generating functionally heterogeneous macrophages: chaos revisited.* J Leukoc Biol, 1993. **53**(5): p. 602-18.

45. Randolph, G.J., *Emigration of monocyte-derived cells to lymph nodes during resolution of inflammation and its failure in atherosclerosis.* Curr Opin Lipidol, 2008. **19**(5): p. 462-8.

46. Fenyo, I.M. and A.V. Gafencu, *The involvement of the monocytes/macrophages in chronic inflammation associated with atherosclerosis.* Immunobiology, 2013. **218**(11): p. 1376-84.

47. Getz, G.S. and C.A. Reardon, *Animal models of atherosclerosis.* Arterioscler Thromb Vasc Biol, 2012. **32**(5): p. 1104-15.

48. Jawien, J., P. Nastalek, and R. Korbut, *Mouse models of experimental atherosclerosis.* J Physiol Pharmacol, 2004. **55**(3): p. 503-17.

49. Plump, A.S., et al., *Severe hypercholesterolemia and atherosclerosis in apolipoprotein E-deficient mice created by homologous recombination in ES cells.* Cell, 1992. **71**(2): p. 343-53.

50. Zhang, S.H., et al., *Spontaneous hypercholesterolemia and arterial lesions in mice lacking apolipoprotein E.* Science, 1992. **258**(5081): p. 468-71.

51. Ishibashi, S., et al., *Massive xanthomatosis and atherosclerosis in cholesterol-fed low density lipoprotein receptor-negative mice.* J Clin Invest, 1994. **93**(5): p. 1885-93.

52. Nakashima, Y., et al., *ApoE-deficient mice develop lesions of all phases of atherosclerosis throughout the arterial tree.* Arterioscler Thromb, 1994. **14**(1): p. 133-40.

53. Allfrey, V.G. and A.E. Mirsky, *Structural Modifications of Histones and their Possible Role in the Regulation of RNA Synthesis.* Science, 1964. **144**(3618): p. 559.

54. Eslaminejad, M.B., N. Fani, and M. Shahhoseini, *Epigenetic regulation of osteogenic and chondrogenic differentiation of mesenchymal stem cells in culture.* Cell J, 2013. **15**(1): p. 1-10.

55. Shakespear, M.R., et al., *Histone deacetylases as regulators of inflammation and immunity.* Trends Immunol, 2011. **32**(7): p. 335-43.

56. Falkenberg, K.J. and R.W. Johnstone, *Histone deacetylases and their inhibitors in cancer, neurological diseases and immune disorders.* Nat Rev Drug Discov, 2014. **13**(9): p. 673-91.

57. Zhou, B., et al., *Role of histone deacetylases in vascular cell homeostasis and arteriosclerosis.* Cardiovasc Res, 2011. **90**(3): p. 413-20.

58. Choudhary, C., et al., *Lysine acetylation targets protein complexes and co-regulates major cellular functions.* Science, 2009. **325**(5942): p. 834-40.

59. Haberland, M., R.L. Montgomery, and E.N. Olson, *The many roles of histone deacetylases in development and physiology: implications for disease and therapy.* Nat Rev Genet, 2009. **10**(1): p. 32-42.

60. McKinsey, T.A., C.L. Zhang, and E.N. Olson, *MEF2: a calcium-dependent regulator of cell division, differentiation and death.* Trends Biochem Sci, 2002. **27**(1): p. 40-7.

61. Fischle, W., et al., *Enzymatic activity associated with class II HDACs is dependent on a multiprotein complex containing HDAC3 and SMRT/N-CoR.* Mol Cell, 2002. **9**(1): p. 45-57.

62. Reddy, D.S., et al., *Measuring Histone Deacetylase Inhibition in the Brain.* Curr Protoc Pharmacol, 2018. **81**(1): p. e41.

63. Li, X., et al., *Methyltransferase Dnmt3a upregulates HDAC9 to deacetylate the kinase TBK1 for activation of antiviral innate immunity.* Nat Immunol, 2016. **17**(7): p. 806-15.

64. Chatterjee, T.K., et al., *Role of histone deacetylase 9 in regulating adipogenic differentiation and high fat diet-induced metabolic disease.* Adipocyte, 2014. **3**(4): p. 333-8.

65. Lapierre, M., et al., *Histone deacetylase 9 regulates breast cancer cell proliferation and the response to histone deacetylase inhibitors.* Oncotarget, 2016. **7**(15): p. 19693-708.

66. Kaluza, D., et al., *Histone deacetylase 9 promotes angiogenesis by targeting the antiangiogenic microRNA-17-92 cluster in endothelial cells.* Arterioscler Thromb Vasc Biol, 2013. **33**(3): p. 533-43.

67. Cao, Q., et al., *Histone deacetylase 9 represses cholesterol efflux and alternatively activated macrophages in atherosclerosis development.* Arterioscler Thromb Vasc Biol, 2014. **34**(9): p. 1871-9.

68. Chen, J., et al., *The Metabolic Regulator Histone Deacetylase 9 Contributes to Glucose Homeostasis Abnormality Induced by Hepatitis C Virus Infection.* Diabetes, 2015. **64**(12): p. 4088-98.

69. Markus, H.S., et al., *Evidence HDAC9 genetic variant associated with ischemic stroke increases risk via promoting carotid atherosclerosis.* Stroke, 2013. **44**(5): p. 1220-5.

70. Zhang, C.L., et al., *Association of COOH-terminal-binding protein (CtBP) and MEF2-interacting transcription repressor (MITR) contributes to transcriptional repression of the MEF2 transcription factor.* J Biol Chem, 2001. **276**(1): p. 35-9.

71. Zhang, C.L., T.A. McKinsey, and E.N. Olson, *The transcriptional corepressor MITR is a signal-responsive inhibitor of myogenesis.* Proc Natl Acad Sci U S A, 2001. **98**(13): p. 7354-9.

72. Zhang, C.L., et al., *Class II histone deacetylases act as signal-responsive repressors of cardiac hypertrophy.* Cell, 2002. **110**(4): p. 479-88.

73. Wang, X.B., et al., *HDAC9 Variant Rs2107595 Modifies Susceptibility to Coronary Artery Disease and the Severity of Coronary Atherosclerosis in a Chinese Han Population.* PLoS One, 2016. **11**(8): p. e0160449.

74. Mihaylova, M.M., et al., *Class IIa histone deacetylases are hormone-activated regulators of FOXO and mammalian glucose homeostasis.* Cell, 2011. **145**(4): p. 607-21.

75. Varga, K., et al., *Histone deacetylase inhibitor- and PMA-induced upregulation of PMCA4b enhances Ca2+ clearance from MCF-7 breast cancer cells.* Cell Calcium, 2014. **55**(2): p. 78-92.

76. Yan, W., et al., *Histone deacetylase inhibitors suppress mutant p53 transcription via histone deacetylase 8.* Oncogene, 2013. **32**(5): p. 599-609.

77. Tao, R., et al., *Deacetylase inhibition promotes the generation and function of regulatory T cells.* Nat Med, 2007. **13**(11): p. 1299-307.

78. Halili, M.A., et al., *Histone deacetylase inhibitors in inflammatory disease.* Curr Top Med Chem, 2009. **9**(3): p. 309-19.

79. Choi, J.H., et al., *Trichostatin A exacerbates atherosclerosis in low density lipoprotein receptor-deficient mice.* Arterioscler Thromb Vasc Biol, 2005. **25**(11): p. 2404-9.

80. Lobera, M., et al., *Selective class IIa histone deacetylase inhibition via a nonchelating zinc-binding group.* Nat Chem Biol, 2013. **9**(5): p. 319-25.

81. Guerriero, J.L., et al., *Class IIa HDAC inhibition reduces breast tumours and metastases through anti-tumour macrophages.* Nature, 2017. **543**(7645): p. 428-432.

82. Sen, R. and D. Baltimore, *Inducibility of kappa immunoglobulin enhancer-binding protein Nf-kappa B by a posttranslational mechanism.* Cell, 1986. **47**(6): p. 921-8.

83. de Winther, M.P., et al., *Nuclear factor kappaB signaling in atherogenesis.* Arterioscler Thromb Vasc Biol, 2005. **25**(5): p. 904-14.

84. Christian, F., E.L. Smith, and R.J. Carmody, *The Regulation of NF-kappaB Subunits by Phosphorylation.* Cells, 2016. **5**(1).

85. Hayden, M.S. and S. Ghosh, *NF-kappaB, the first quarter-century: remarkable progress and outstanding questions.* Genes Dev, 2012. **26**(3): p. 203-34.

86. Baker, R.G., M.S. Hayden, and S. Ghosh, *NF-kappaB, inflammation, and metabolic disease.* Cell Metab, 2011. **13**(1): p. 11-22.

87. Courtois, G. and T.D. Gilmore, *Mutations in the NF-kappaB signaling pathway: implications for human disease.* Oncogene, 2006. **25**(51): p. 6831-43.

88. Karin, M., *Nuclear factor-kappaB in cancer development and progression.* Nature, 2006. **441**(7092): p. 431-6.

89. Hayden, M.S. and S. Ghosh, *Shared principles in NF-kappaB signaling.* Cell, 2008. **132**(3): p. 344-62.

90. Oeckinghaus, A., M.S. Hayden, and S. Ghosh, *Crosstalk in NF-kappaB signaling pathways.* Nat Immunol, 2011. **12**(8): p. 695-708.

91. Chen, Z., et al., *Signal-induced site-specific phosphorylation targets I kappa B alpha to the ubiquitin-proteasome pathway.* Genes Dev, 1995. **9**(13): p. 1586-97.

92. Ruland, J., *Return to homeostasis: downregulation of NF-kappaB responses.* Nat Immunol, 2011. **12**(8): p. 709-14.

93. Sun, S.C., et al., *NF-kappa B controls expression of inhibitor I kappa B alpha: evidence for an inducible autoregulatory pathway.* Science, 1993. **259**(5103): p. 1912-5.

94. Arenzana-Seisdedos, F., et al., *Inducible nuclear expression of newly synthesized I kappa B alpha negatively regulates DNA-binding and transcriptional activities of NF-kappa B.* Mol Cell Biol, 1995. **15**(5): p. 2689-96.

95. Zhong, H., et al., *The phosphorylation status of nuclear NF-kappa B determines its association with CBP/p300 or HDAC-1.* Mol Cell, 2002. **9**(3): p. 625-36.

96. Chen, L., et al., *Duration of nuclear NF-kappaB action regulated by reversible acetylation.* Science, 2001. **293**(5535): p. 1653-7.

97. Ashburner, B.P., S.D. Westerheide, and A.S. Baldwin, Jr., *The p65 (RelA) subunit of NF-kappaB interacts with the histone deacetylase (HDAC) corepressors HDAC1 and HDAC2 to negatively regulate gene expression.* Mol Cell Biol, 2001. **21**(20): p. 7065-77.

98. Moreno, R., et al., *Specification of the NF-kappaB transcriptional response by p65 phosphorylation and TNF-induced nuclear translocation of IKK epsilon.* Nucleic Acids Res, 2010. **38**(18): p. 6029-44.

99. Gardam, S. and R. Brink, *Non-Canonical NF-kappaB Signaling Initiated by BAFF Influences B Cell Biology at Multiple Junctures.* Front Immunol, 2014. **4**: p. 509.

100. Buss, H., et al., *Constitutive and interleukin-1-inducible phosphorylation of p65 NF-{kappa}B at serine 536 is mediated by multiple protein kinases including I{kappa}B kinase (IKK)-{alpha}, IKK{beta}, IKK{epsilon}, TRAF family member-*

associated (TANK)-binding kinase 1 (TBK1), and an unknown kinase and couples p65 to TATA-binding protein-associated factor II31-mediated interleukin-8 transcription. J Biol Chem, 2004. **279**(53): p. 55633-43.

101. Chen, L.F., et al., *NF-kappaB RelA phosphorylation regulates RelA acetylation.* Mol Cell Biol, 2005. **25**(18): p. 7966-75.

102. Buss, H., et al., *Phosphorylation of serine 468 by GSK-3beta negatively regulates basal p65 NF-kappaB activity.* J Biol Chem, 2004. **279**(48): p. 49571-4.

103. Mattioli, I., et al., *Inducible phosphorylation of NF-kappa B p65 at serine 468 by T cell costimulation is mediated by IKK epsilon.* J Biol Chem, 2006. **281**(10): p. 6175-83.

104. Schwabe, R.F. and H. Sakurai, *IKKbeta phosphorylates p65 at S468 in transactivaton domain 2.* FASEB J, 2005. **19**(12): p. 1758-60.

105. Geng, H., et al., *Phosphorylation of NF-kappaB p65 at Ser468 controls its COMMD1-dependent ubiquitination and target gene-specific proteasomal elimination.* EMBO Rep, 2009. **10**(4): p. 381-6.

106. Sakurai, H., et al., *IkappaB kinases phosphorylate NF-kappaB p65 subunit on serine 536 in the transactivation domain.* J Biol Chem, 1999. **274**(43): p. 30353-6.

107. Lawrence, T., et al., *IKKalpha limits macrophage NF-kappaB activation and contributes to the resolution of inflammation.* Nature, 2005. **434**(7037): p. 1138-43.

108. Bao, X., et al., *IKKepsilon modulates RSV-induced NF-kappaB-dependent gene transcription.* Virology, 2010. **408**(2): p. 224-31.

109. Asare, Y., et al., *Inhibition of atherogenesis by the COP9 signalosome subunit 5 in vivo.* Proc Natl Acad Sci U S A, 2017. **114**(13): p. E2766-E2775.

110. Ngkelo, A., et al., *LPS induced inflammatory responses in human peripheral blood mononuclear cells is mediated through NOX4 and Gialpha dependent PI-3kinase signalling.* J Inflamm (Lond), 2012. **9**(1): p. 1.

111. Bouwmeester, T., et al., *A physical and functional map of the human TNF-alpha/NF-kappa B signal transduction pathway.* Nat Cell Biol, 2004. **6**(2): p. 97-105.

112. Parameswaran, N. and S. Patial, *Tumor necrosis factor-alpha signaling in macrophages.* Crit Rev Eukaryot Gene Expr, 2010. **20**(2): p. 87-103.

113. Maskrey, B.H., et al., *Mechanisms of resolution of inflammation: a focus on cardiovascular disease.* Arterioscler Thromb Vasc Biol, 2011. **31**(5): p. 1001-6.

114. Geovanini, G.R. and P. Libby, *Atherosclerosis and inflammation: overview and updates.* Clin Sci (Lond), 2018. **132**(12): p. 1243-1252.

115. Aung, H.T., et al., *LPS regulates proinflammatory gene expression in macrophages by altering histone deacetylase expression.* FASEB J, 2006. **20**(9): p. 1315-27.

116. Ziesche, E., et al., *The coactivator role of histone deacetylase 3 in IL-1-signaling involves deacetylation of p65 NF-kappaB.* Nucleic Acids Res, 2013. **41**(1): p. 90-109.

117. Bhaskar, V., et al., *Monoclonal antibodies targeting IL-1 beta reduce biomarkers of atherosclerosis in vitro and inhibit atherosclerotic plaque formation in Apolipoprotein E-deficient mice.* Atherosclerosis, 2011. **216**(2): p. 313-20.

118. Xiao, N., et al., *Tumor necrosis factor-alpha deficiency retards early fatty-streak lesion by influencing the expression of inflammatory factors in apoE-null mice.* Mol Genet Metab, 2009. **96**(4): p. 239-44.

119. Branen, L., et al., *Inhibition of tumor necrosis factor-alpha reduces atherosclerosis in apolipoprotein E knockout mice.* Arterioscler Thromb Vasc Biol, 2004. **24**(11): p. 2137-42.

120. Ohta, H., et al., *Disruption of tumor necrosis factor-alpha gene diminishes the development of atherosclerosis in ApoE-deficient mice.* Atherosclerosis, 2005. **180**(1): p. 11-7.

121. Huber, S.A., et al., *Interleukin-6 exacerbates early atherosclerosis in mice.* Arterioscler Thromb Vasc Biol, 1999. **19**(10): p. 2364-7.

122. Schieffer, B., et al., *Impact of interleukin-6 on plaque development and morphology in experimental atherosclerosis.* Circulation, 2004. **110**(22): p. 3493-500.

123. Madan, M., et al., *Atheroprotective role of interleukin-6 in diet- and/or pathogen-associated atherosclerosis using an ApoE heterozygote murine model.* Atherosclerosis, 2008. **197**(2): p. 504-14.

124. Richmond, A., *Nf-kappa B, chemokine gene transcription and tumour growth.* Nat Rev Immunol, 2002. **2**(9): p. 664-74.

125. Kanters, E., et al., *Inhibition of NF-kappaB activation in macrophages increases atherosclerosis in LDL receptor-deficient mice.* J Clin Invest, 2003. **112**(8): p. 1176-85.

126. Fitzgerald, K.A., et al., *IKKepsilon and TBK1 are essential components of the IRF3 signaling pathway.* Nat Immunol, 2003. **4**(5): p. 491-6.

127. Adam, E., et al., *Potentiation of tumor necrosis factor-induced NF-kappa B activation by deacetylase inhibitors is associated with a delayed cytoplasmic reappearance of I kappa B alpha.* Mol Cell Biol, 2003. **23**(17): p. 6200-9.

128. Myasoedova, V.A., et al., *Inhibitors of DNA Methylation and Histone Deacetylation as Epigenetically Active Drugs for Anticancer Therapy.* Curr Pharm Des, 2019. **25**(6): p. 635-641.

129. Van den Bossche, J., et al., *Inhibiting epigenetic enzymes to improve atherogenic macrophage functions.* Biochem Biophys Res Commun, 2014. **455**(3-4): p. 396-402.

130. Zampetaki, A., et al., *Histone deacetylase 3 is critical in endothelial survival and atherosclerosis development in response to disturbed flow.* Circulation, 2010. **121**(1): p. 132-42.

131. Hoeksema, M.A., et al., *Targeting macrophage Histone deacetylase 3 stabilizes atherosclerotic lesions.* EMBO Mol Med, 2014. **6**(9): p. 1124-32.

132. Grabiec, A.M., et al., *Histone deacetylase inhibitors suppress rheumatoid arthritis fibroblast-like synoviocyte and macrophage IL-6 production by accelerating mRNA decay.* Ann Rheum Dis, 2012. **71**(3): p. 424-31.

133. Han, S.B. and J.K. Lee, *Anti-inflammatory effect of Trichostatin-A on murine bone marrow-derived macrophages.* Arch Pharm Res, 2009. **32**(4): p. 613-24.

134. Leoni, F., et al., *The histone deacetylase inhibitor ITF2357 reduces production of pro-inflammatory cytokines in vitro and systemic inflammation in vivo.* Mol Med, 2005. **11**(1-12): p. 1-15.

135. Usami, M., et al., *Butyrate and trichostatin A attenuate nuclear factor kappaB activation and tumor necrosis factor alpha secretion and increase prostaglandin E2 secretion in human peripheral blood mononuclear cells.* Nutr Res, 2008. **28**(5): p. 321-8.

136. Federico, M. and L. Bagella, *Histone deacetylase inhibitors in the treatment of hematological malignancies and solid tumors.* J Biomed Biotechnol, 2011. **2011**: p. 475641.

9 Acknowledgements

First and foremost, I would like to sincerely thank my mentor Dr. rer. nat. Yaw Asare for teaching me everything in the process of this thesis, for all his knowledge and skills in the lab and for all the invested time, help and ideas. I am very grateful for all your help.

Furthermore, I would like to sincerely thank my doctoral supervisor Prof. Martin Dichgans for enabling this opportunity at the institute, for the ideas and input and for showing interest in this thesis.

Also, I would like to thank all of AG Dichgans, especially Melanie Schneider for all the perfect organization and Natalie Ziesch for all the help with the experiments. Also, many thanks to all the other MD students who became good friends also outside of the lab.

And lastly, I would like to thank my family and my boyfriend; without their support and encouraging words I would not be where I am today.